Earth's Ionosphere and Atmosphere

Tim Fuller-Rowell
CIRES, University of Colorado and
Space Weather Prediction Center, NOAA

With thanks to Jeffrey Thayer for some ionospheric slides

University of Colorado
Boulder

Contents: Temperature, Composition, Dynamics

Electrodynamics –refer to Heelis tutorial

Recommended reading/listening

- Heliophysics book Volume 1 Ch 12
- Heliophysics book Volume 2 Ch 12
- Heliophysics Tutorials by Heelis, Solomon, Sojka
- AGU Monograph 201: Modeling the Ionosphere Thermosphere System

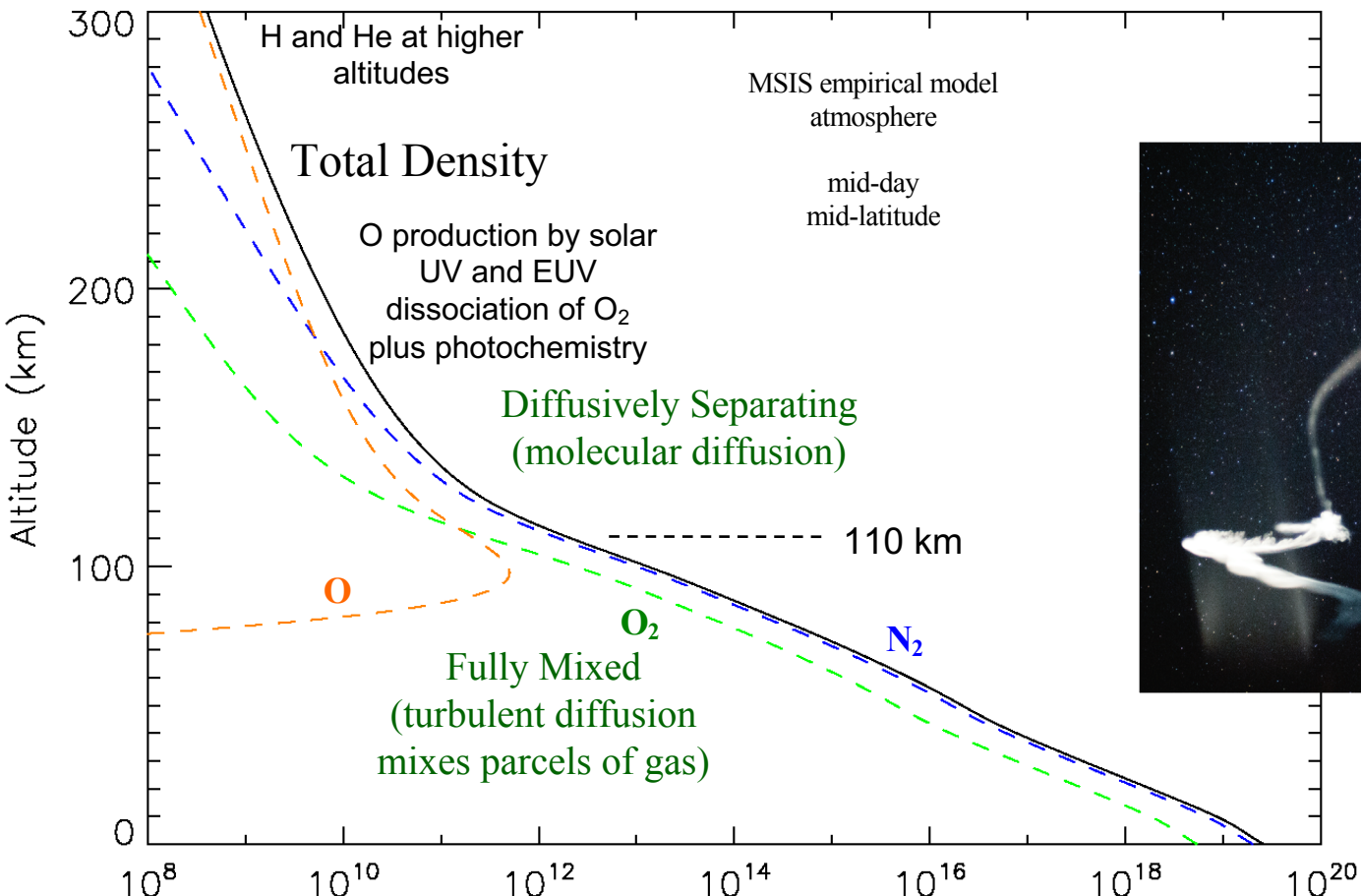# Upper Atmosphere Space Weather Impacts on Operational Systems

- Neutral density

  - Satellite drag in low-Earth orbit (LEO): space traffic management, orbit prediction, conjunction prediction, collision avoidance, re-entry (neutral mass density, winds, structure, waves)

- Ionosphere – impacts radio wave propagation

  - HF *communications* 3 – 30 MHz: D-region absorbs signal; F-layer reflects/ refracts signal; structure, gradients, undulations, and tilts scatter signals

  - GNSS precise point *positioning*, satellite *navigation*, and *timing* (PNT; GPS 1575 and 1228 MHz): line of sight total electron content delays and refracts signals; plasma irregularities, structure and gradients diffract signals, causing amplitude and phase scintillations and sometime complete loss of signal

  - Satellite *communications*: plasma irregularities cause scintillations and loss of signal
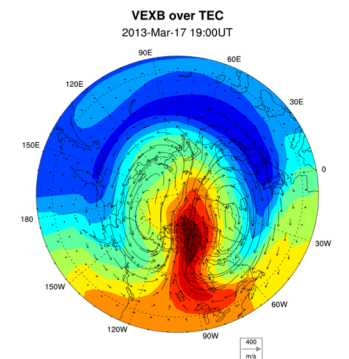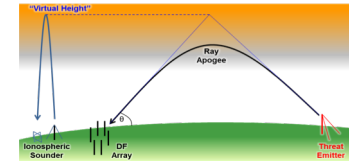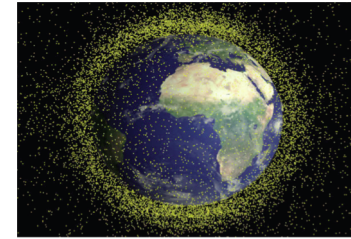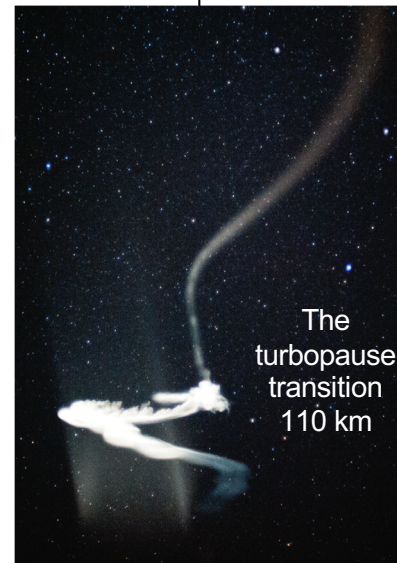
Earth's Neutral Thermosphere/Atmosphere

- Gravitationally bound
- Collision dominated - kinetic theory, fluid properties up to ~600 km, Navier Stokes, gas laws
- Partially (singly) ionized < 1% (100-600km altitude)
- Magnetic field - 99% invariant on short timescales

Major Species Density Structure of the Atmosphere

H and He at higher altitudes

Total Density

O production by solar UV and EUV dissociation of O_2 plus photochemistry

MSIS empirical model atmosphere

mid-day
mid-latitude

Diffusively Separating
(molecular diffusion)

- - - - - - - 110 km

O

O₂

N₂
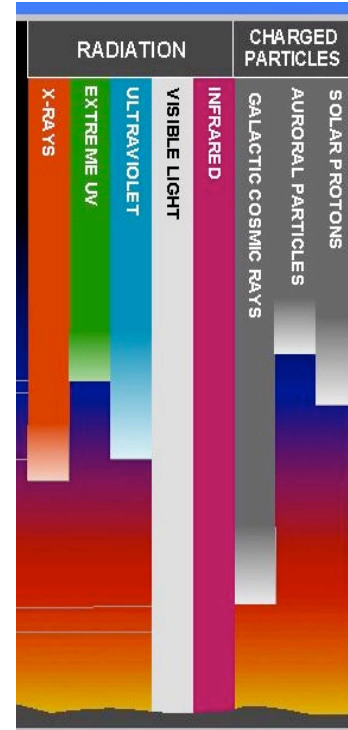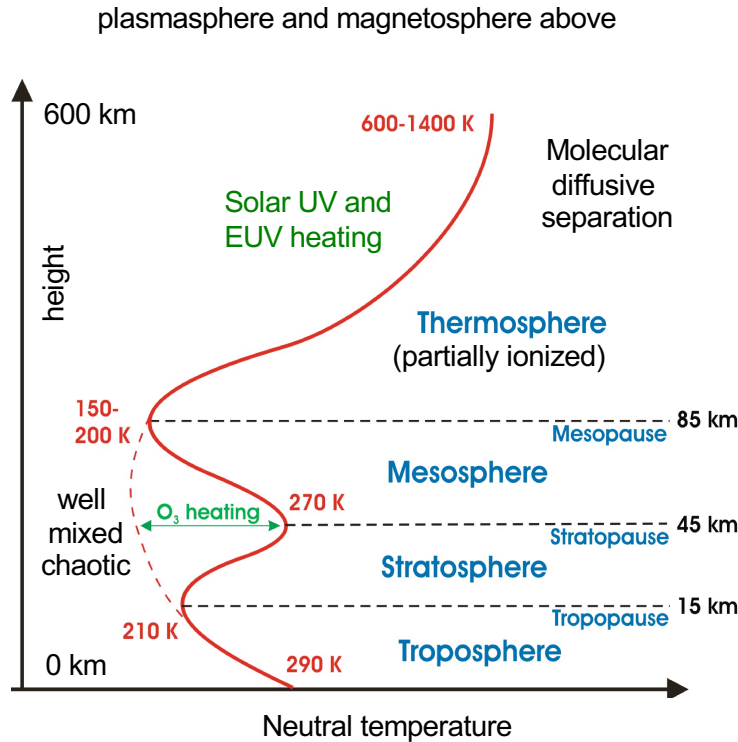
Fully Mixed
(turbulent diffusion mixes parcels of gas)
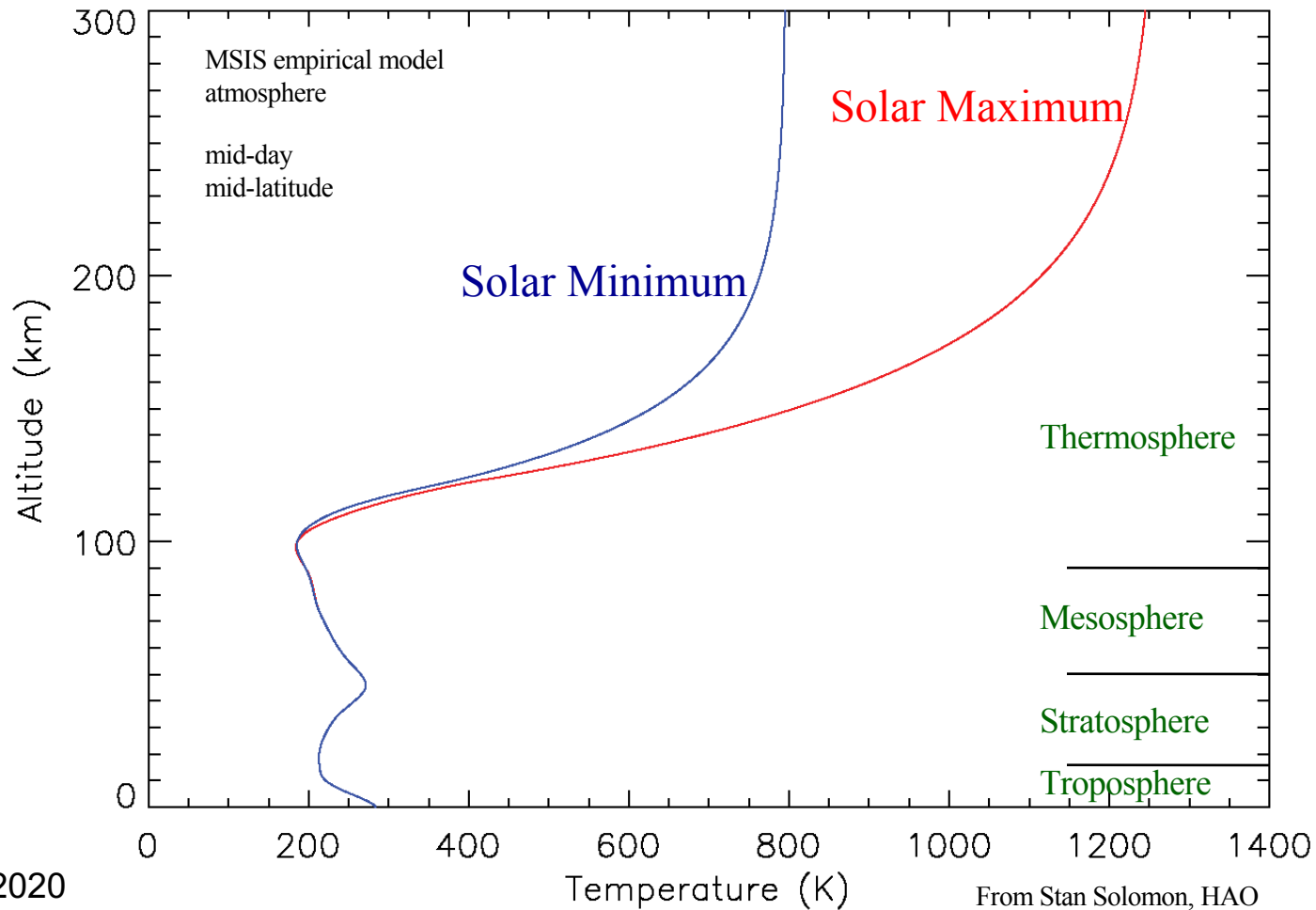
Turbopause –
transition from chaotic regime

Laminar flow above the turbopause with molecular diffusion - separation of heavy and light species in altitude but with wave and circulation mixing

The turbopause transition 110 km

Gravity wave breaking and well mixed below the turbopause height near ~110 km

Altitude (km)

Density (cm⁻³)

Heliophysics Summer School I-T

Earth's Temperature Structure

July 16th, 2020   Heliophysics Summer School I-T

Temperature Structure – Solar Cycle Variation

MSIS empirical model atmosphere

mid-day mid-latitude

Solar Maximum

Solar Minimum

Thermosphere

Mesosphere

Stratosphere

Troposphere

Altitude (km)

Temperature (K)

July 16th, 2020

From Stan Solomon, HAO

Atmospheric Distribution in Hydrostatic Equilibrium

Pressure gradient:
$$\frac{dp}{dz} = -g(z)\rho$$

(height derivative of pressure equals acceleration of gravity times density)

Perfect gas law:
$$p = nkT = \frac{\rho}{M}kT$$

M is the mean molecular mass

If g and T are not functions of z, then:
$$\frac{dp}{dz} = -p\frac{Mg}{kT} = -\frac{p}{H}$$

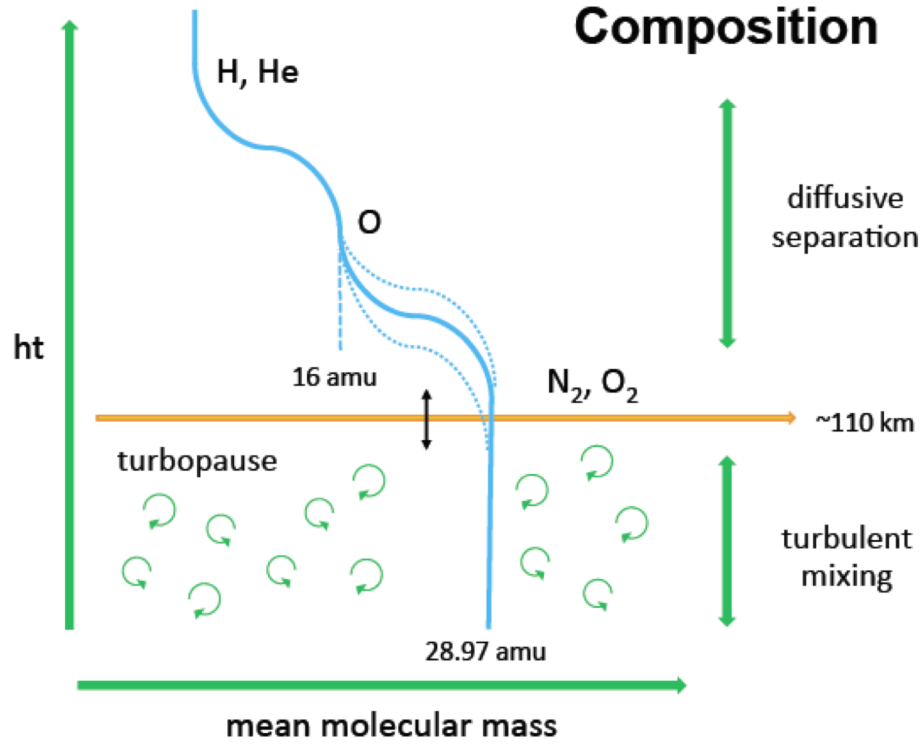where scale height $H = \frac{kT}{Mg}$

$$\frac{dp}{p} = -\frac{dz}{H}$$

"law of atmospheres":
$$p(z) = p(z_0)\exp\left[-\frac{z - z_0}{H}\right]$$

In diffusive separation:
$$n_j(z) = n_j(z_0)\exp\left[-\frac{z - z_0}{H_j}\right]$$

where $H_j = \frac{kT}{M_j g}$

13

8

$$\frac{\partial \psi_i}{\partial t} = \frac{1}{\rho} m S_i - \nabla \cdot \nabla p \psi_i - \omega \frac{\partial}{\partial p} \psi_i - \frac{1}{\rho} \nabla \cdot (n_i m C_i) + \frac{1}{\rho} \frac{\partial}{\partial p} \left(K_T \frac{\partial}{\partial p} m \psi_i \right)$$
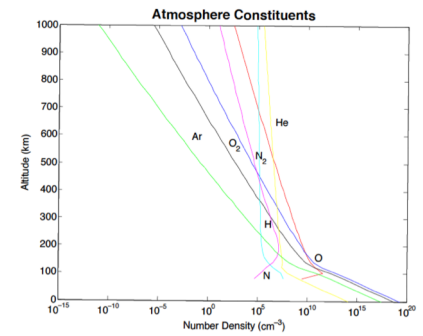
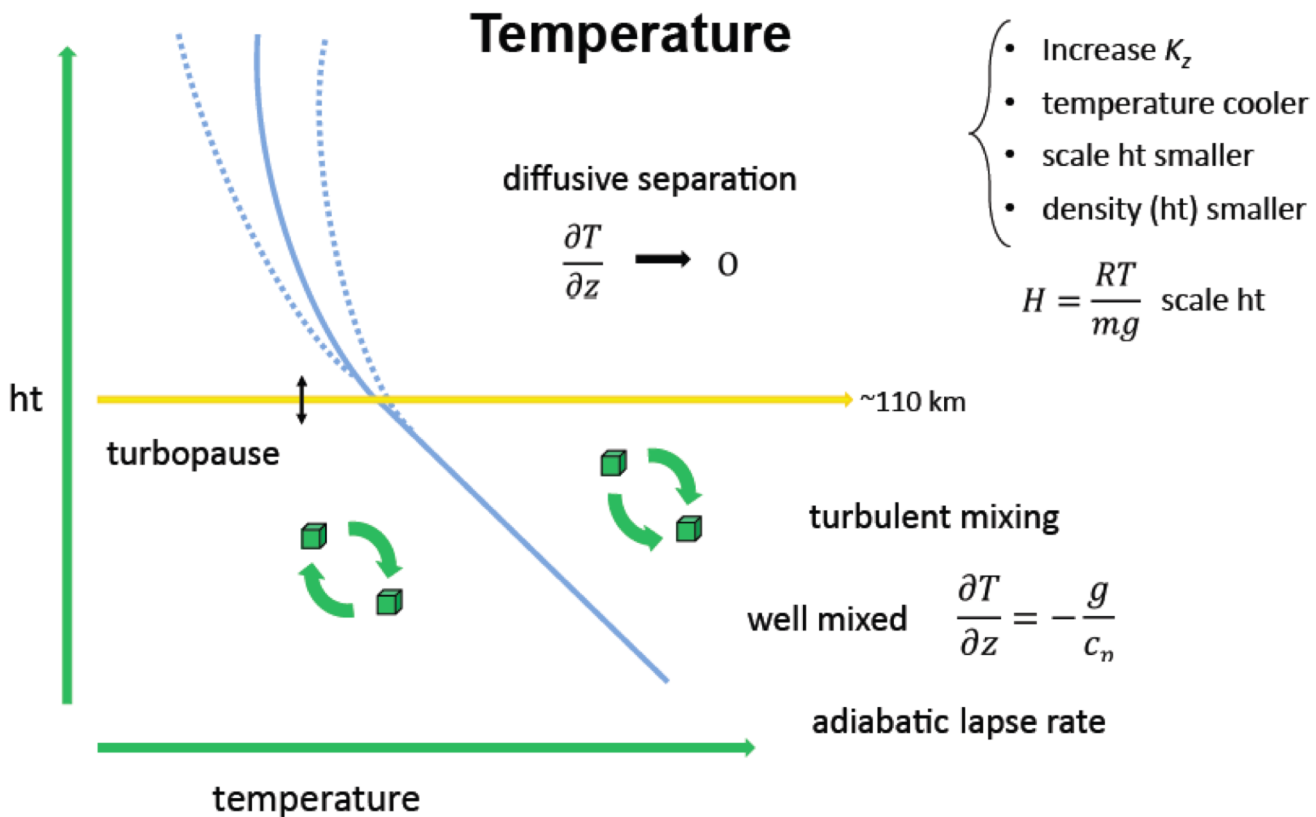Ψ_i – species mixing ratios

eddy mixing

Composition

H, He

O

16 amu

N$_2$, O$_2$

ht

~110 km

diffusive separation

turbulent mixing

turbopause

28.97 amu

mean molecular mass

- Increase K_z
- Turbopause higher
- More mixing
- O/N$_2$ small
- Scale ht smaller
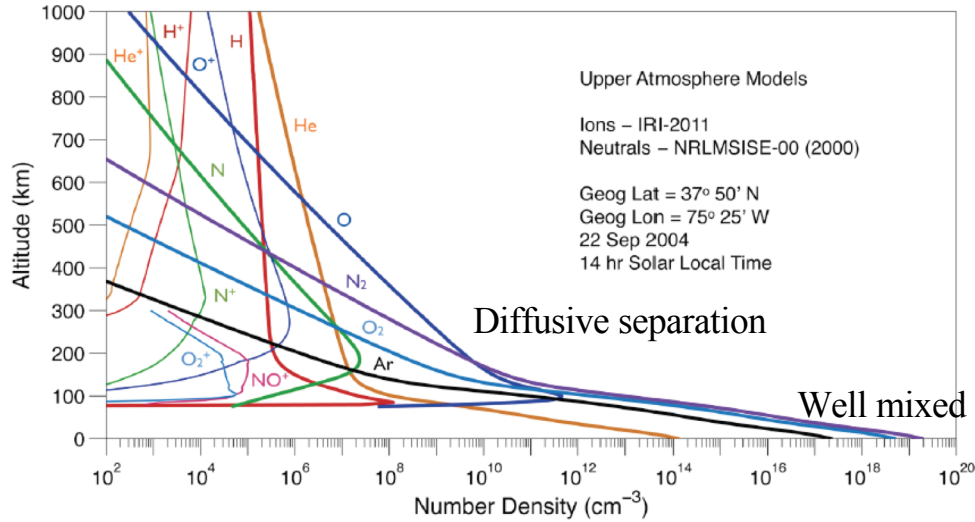- Density (ht) smaller

$H = \dfrac{RT}{mg}$ scale ht

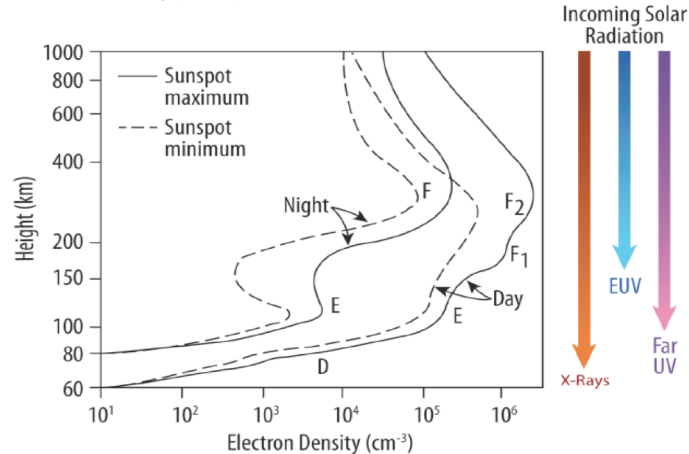Atmosphere Constituents

Vertical heat conduction

$$g \frac{\partial}{\partial p}\left[\left(\kappa_m + \kappa_T\right) \frac{p}{H} \frac{\partial}{\partial p} T\right] - g \frac{\partial}{\partial p} \frac{g\kappa_T}{c_p}$$

Temperature

diffusive separation

$$\frac{\partial T}{\partial z} \longrightarrow 0$$

- Increase K_z
- temperature cooler
- scale ht smaller
- density (ht) smaller

$$H = \frac{RT}{mg} \quad \text{scale ht}$$

ht ————————————————————— ~110 km

turbopause

turbulent mixing

well mixed $\quad \dfrac{\partial T}{\partial z} = -\dfrac{g}{c_n}$

adiabatic lapse rate

temperature

Diffusive separation in the upper atmosphere

Upper Atmosphere Models

Ions – IRI-2011
Neutrals – NRLMSISE-00 (2000)

Geog Lat = 37° 50' N
Geog Lon = 75° 25' W
22 Sep 2004
14 hr Solar Local Time

Diffusive separation

Well mixed

Plasma is space weather's water vapor: <1% plasma

Solar Radiation – Photoionization and Dissociation

Photon energy in eV = hc/λ

- Photodissociation $\quad(\lambda \leq 242nm)$

  $$O_2 + photon(\lambda \leq 242nm) \rightarrow O + O$$

- Photoionization $\quad(\lambda \leq 103nm)$

  $$O + photon(\lambda \leq 91nm) \rightarrow O^+ + e$$

  $$N_2 + photon(\lambda \leq 80nm) \rightarrow N_2^+ + e$$

  $$O_2 + photon(\lambda \leq 103nm) \rightarrow O_2^+ + e$$

- Dissociative Photoionization $\quad(\lambda \leq 72nm)$

  $$N_2 + photon(\lambda \leq 49nm) \rightarrow N^+ + N + e$$
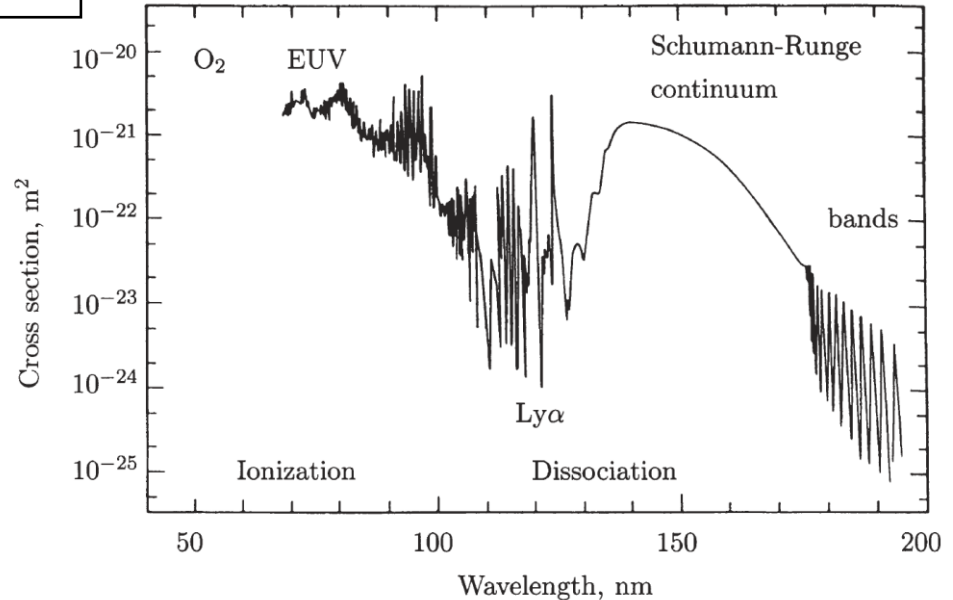
Fig. 3.12. Absorption cross section of molecular oxygen at wavelengths 70-195 nm. The absorption is dominated by ionization below $\lambda \simeq 103$ nm and by dissociation above this wavelength (adapted from Banks and Kockarts, 1973).

Altitude of Maximum Solar Radiation Absorption
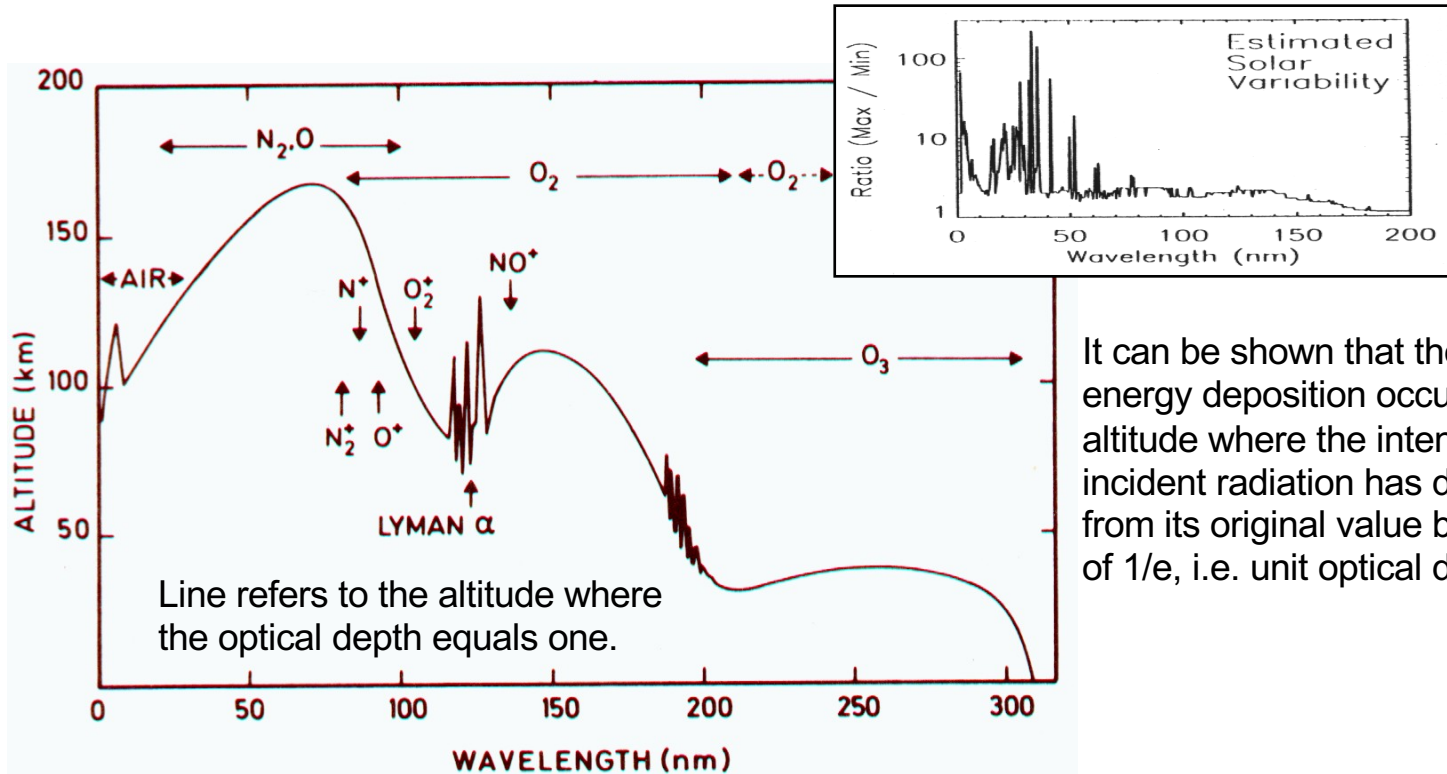
It can be shown that the maximal energy deposition occurs at that altitude where the intensity of the incident radiation has decreased from its original value by a factor of 1/e, i.e. unit optical depth.

Line refers to the altitude where the optical depth equals one.

Solar Flux Energy Deposition Rate per unit Volume [W/m³]
Chapman Production Function
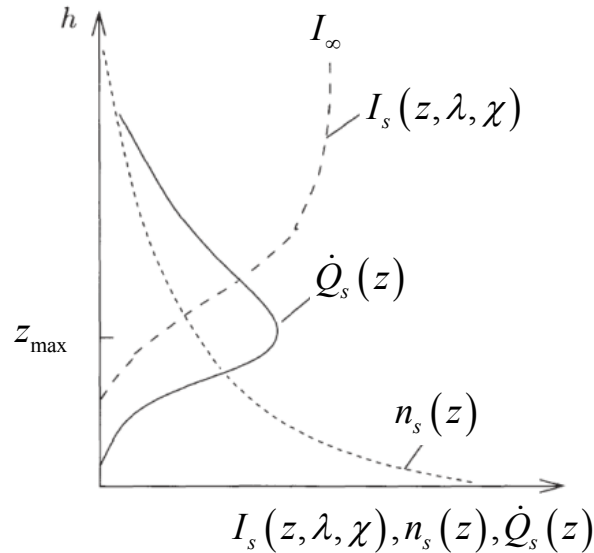
Fig. 4.4. Formation of ionization production layers

Photon flux, number of photons per area per time

$$I(s_\lambda) = I_\infty(\lambda) e^{-\tau(s)}$$

Photons absorbed at altitude, z_0, per unit volume element per unit time

$$\frac{dI(s_\lambda)}{ds}\bigg|_z = -\sigma^A n(z_0) I(z_0)$$

Energy deposition at altitude, z_0, per unit volume element per unit time

$$\dot{Q}_s(z_0) = \sigma(\lambda)^A n_s(z_0) I_s(z_0, \lambda, \chi)\left(\frac{hc}{\lambda}\right) = \sigma(\lambda)^A n_s(z_0) I_\infty(\lambda)\left(\frac{hc}{\lambda}\right) e^{-\tau(z_0)}$$

Where the absorption cross section is the sum of the probabilities that an absorption "collision" will produce photodissociation, photoionization, and other processes.

Chapman Production Function

$$\dot{Q}_s(z) = \dot{Q}_{s,max} \exp\left\{1 - \frac{z - z_{max}}{H} - \sec\chi \exp\left(\frac{-(z - z_{max})}{H}\right)\right\}$$

Height

+4H

+3H

+2H

+1H

$\chi = 75°$ $\chi = 0°$

$z_{max} = z_{abs}(\tau = 1)$

0.2 0.4 0.6 0.8 1

$\dfrac{\dot{Q}_s(z, \chi = 0°)}{\dot{Q}_{s,max}(\chi = 0°)}$

−1H

−2H
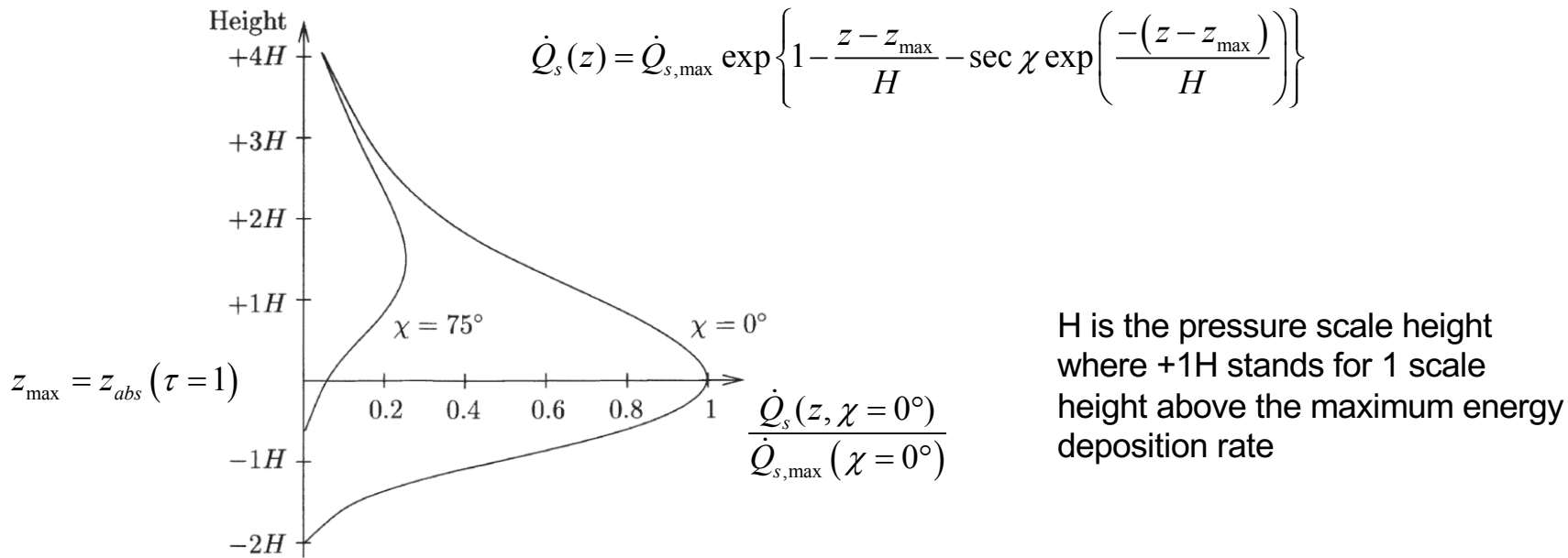
Fig. 3.18. Chapman production function for two different solar zenith angles.

H is the pressure scale height where +1H stands for 1 scale height above the maximum energy deposition rate

Energy Distribution of Solar EUV Flux into the Thermosphere
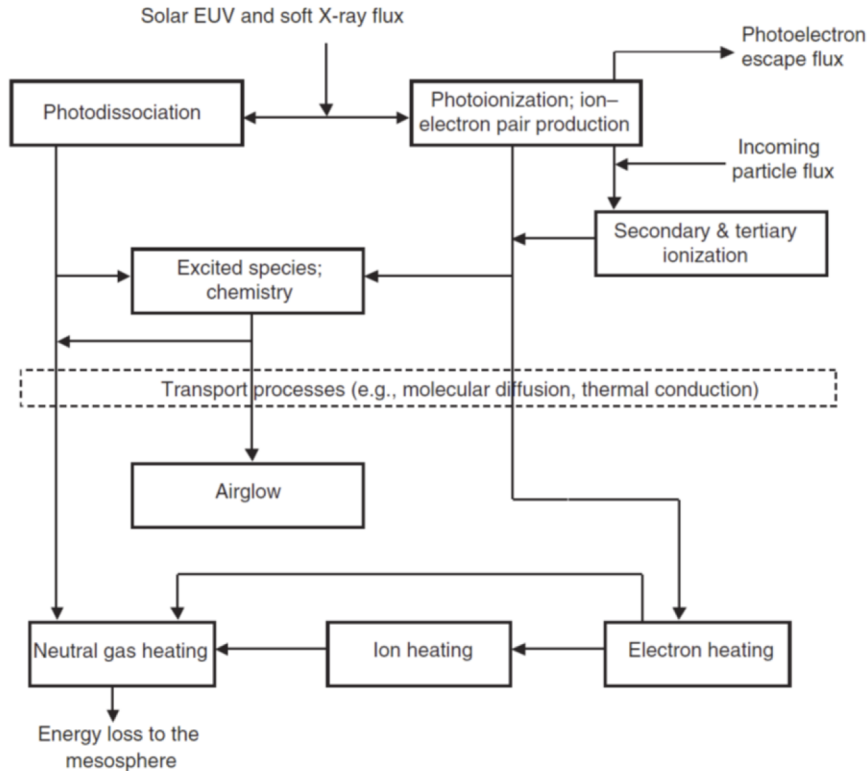
Neutral, Ion and Electron Temperature Profile
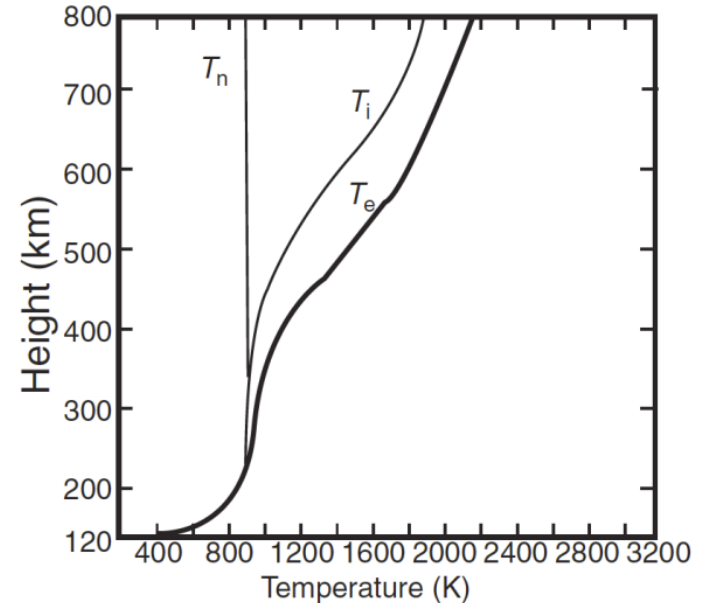
Figure 9.1 Block diagram of the energy flow in the upper atmosphere.

Ion Production Rate
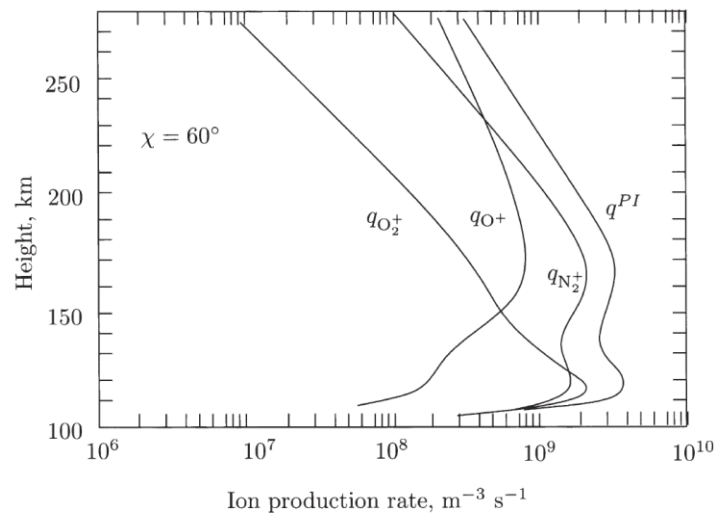
Fig. 4.5. Representative production profiles for the most important ions from primary photoionization and their sum q^{PI}. As earlier, χ denotes the zenith angle of the incident radiation (adapted from Matuura, 1966).

Net ion production deviates from the generalized Chapman Layer due to multiconstituent and polychromatic radiation
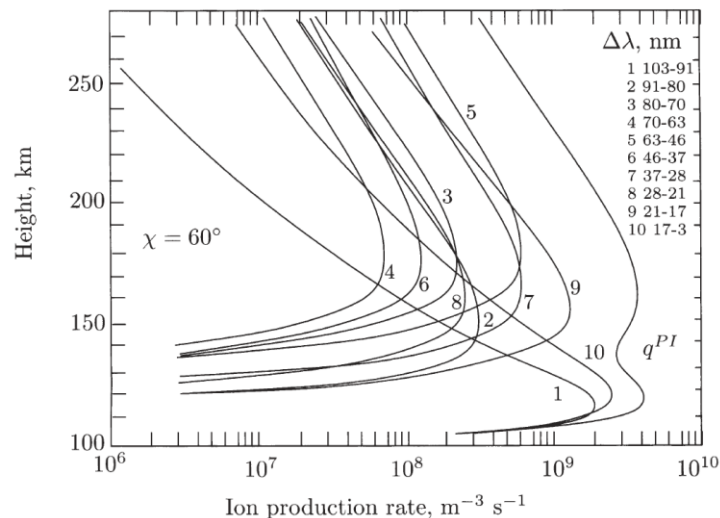
Fig. 4.6. Ionization production profiles for various wavelength ranges (see also Fig. 4.5, adapted from Matuura, 1966)

17

Ionization Rate due to Monoenergetic Electron Flux (Auroral)
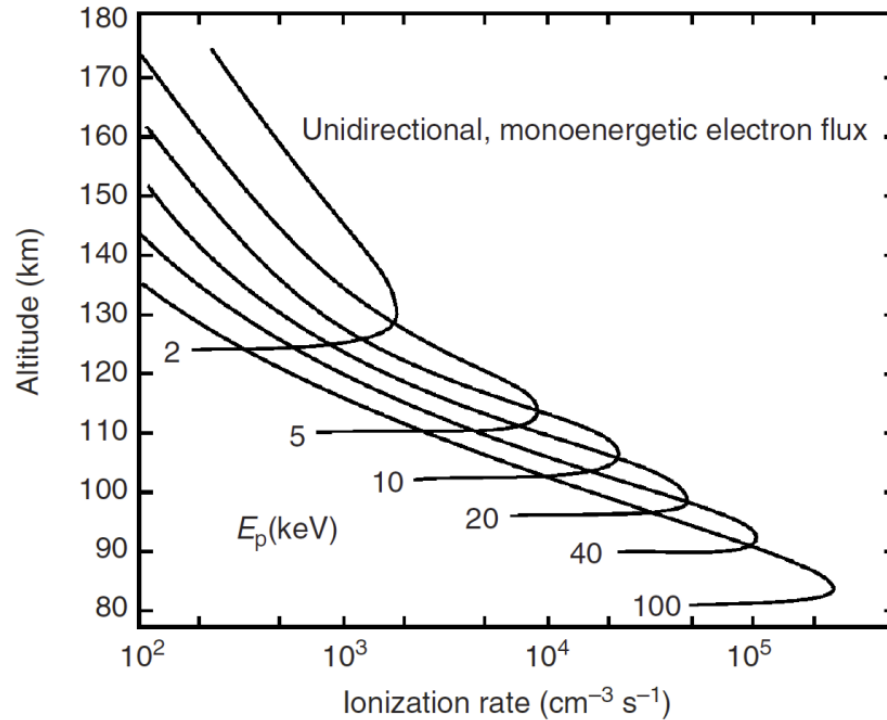
Figure 9.7 Calculated electron–ion pair production rates for monoenergetic electron fluxes of 10^8 electrons cm^{-2} s^{-1} precipitating into the terrestrial atmosphere.[22]

Ionosphere Chemical Reactions

Table 4.3. Important chemical reactions in the ionosphere (adapted from Schunk, 1983)

(1) $O^+ + N_2 \longrightarrow NO^+ + N,$

$k_1 = 1.533 \cdot 10^{-18} - 5.92 \cdot 10^{-19} (T/300) + 8.60 \cdot 10^{-20} (T/300)^2 ;$

$$300 \leq T \leq 1700 \text{ K}$$

$k_1 = 2.73 \cdot 10^{-18} - 1.155 \cdot 10^{-18} (T/300) + 1.483 \cdot 10^{-19} (T/300)^2 ;$

$$1700 < T \leq 6000 \text{ K}$$

(2) $O^+ + O_2 \longrightarrow O_2^+ + O,$

$k_2 = 2.82 \cdot 10^{-17} - 7.74 \cdot 10^{-18} (T/300) + 1.073 \cdot 10^{-18} (T/300)^2$

$- 5.17 \cdot 10^{-20} (T/300)^3 + 9.65 \cdot 10^{-22} (T/300)^4; \ 300 \leq T \leq 6000 \text{ K}$

(3) $O^+ + H \rightleftharpoons H^+ + O, \quad \overrightarrow{k}_3 = 2.5 \cdot 10^{-17} \sqrt{T_n}$

$$\overleftarrow{k}_3 = 2.2 \cdot 10^{-17} \sqrt{T_i}$$

(4) $N_2^+ + O_2 \longrightarrow O_2^+ + N_2, \quad k_4 = 5 \cdot 10^{-17} (300/T)$

(5) $N_2^+ + O \longrightarrow O^+ + N_2, \quad k_5 = 1 \cdot 10^{-17} (300/T)^{0.23} ;$

$$T \leq 1500 \text{ K}$$

(6) $N_2^+ + O \longrightarrow NO^+ + N, \quad k_6 = 1.4 \cdot 10^{-16} (300/T)^{0.44} ;$

$$T \leq 1500 \text{ K}$$

(7) $N^+ + O_2 \longrightarrow NO^+ + O, \quad k_7 = 2.6 \cdot 10^{-16}$

(8) $N^+ + O_2 \longrightarrow O_2^+ + N, \quad k_8 = 3.1 \cdot 10^{-16}$

(9) $He^+ + N_2 \longrightarrow N^+ + He + N, \quad k_9 = 9.6 \cdot 10^{-16}$

(10) $He^+ + N_2 \longrightarrow N_2^+ + He, \quad k_{10} = 6.4 \cdot 10^{-16}$

(11) $He^+ + O_2 \longrightarrow O^+ + He + O, \quad k_{11} = 1.1 \cdot 10^{-15}$

(12) $N_2^+ + e \longrightarrow N + N, \quad k_{12} = 1.8 \cdot 10^{-13} (300/T_e)^{0.39}$

(13) $O_2^+ + e \longrightarrow O + O, \quad k_{13} = 1.6 \cdot 10^{-13} (300/T_e)^{0.55}$

(14) $NO^+ + e \longrightarrow N + O, \quad k_{14} = 4.2 \cdot 10^{-13} (300/T_e)^{0.85}$

(15) $O^+ + e \longrightarrow O^{(*)} + h\nu, \quad k_{15} \simeq 1.4 \cdot 10^{-18} (1160/T_e)^{0.5}$

where the reaction constants k_i are in $[\text{m}^3\text{s}^{-1}]$, $T \simeq T_n$ for small ion drift velocities and $T_i \simeq T_n$. In the presence of polar electric fields, the temperature in the F region increases as $T[\text{K}] \simeq T_n[\text{K}] + 0.33 \, \mathcal{E}_{eff}^2[\text{mV/m}]$, where $\vec{\mathcal{E}}_{eff} = \vec{\mathcal{E}}_\perp + \vec{u}_n \times \vec{B}$ ($\vec{\mathcal{E}}_\perp =$ externally applied electric field component perpendicular to the magnetic field $\vec{B}$, $\vec{u}_n =$ neutral gas velocity and $\vec{B} =$ geomagnetic field vector; see also Section 7.5.2).

Many of the bi-products of photoionization and photochemistry are a source of O

Ionospheric Chemistry Processes

- Dissociative Recombination of <u>Molecular</u> Ions

$$XY^+ + e \rightarrow X + Y \ , \ k_{12-14}^{DR} \ \left(Fast \right) \qquad \text{Reactions 12-14}$$

- Radiative Recombination of <u>Atomic</u> Ions

$$X^+ + e \rightarrow X + h\nu \ , \ k_{15}^{RR} \ (Slow) \qquad \text{Reaction 15}$$

- Charge Exchange or Rearrangement of Charge

$$X^+ + Y \rightarrow X + Y^+ \ , \ k_{2-5}^{CE} \ \left(Slow \text{ but high number of reactants} \right) \quad \text{Reactions 1-11}$$

Dynamics of Chemical Species

Three different cases can be identified in the ionosphere to characterize the effects of the competition between dynamics and chemistry - in terms of time constants τ

- $\tau_{chem} \gg \tau_{dyn}$. Here, dynamics will serve to control the species distribution, eliminate gradients and potentially mix with other species. [Topside F region]

- $\tau_{chem} \sim \tau_{dyn}$. Both processes are at play and require a complete coupled analysis of the chemistry and dynamics. [F-region peak]

- $\tau_{chem} \ll \tau_{dyn}$. Under these circumstances, the species in question will be in photochemical equilibrium. Dynamics may still be important indirectly via the effects of temperature or coupling between species. [E-region and lower F-region]

F-region [O+ Dominant] Ionosphere

$$[O^+] = [N_e]$$

F Region

$$P_{O^+} = q(O^+)$$

Ion production by photo-ionization

Ne loss by chemistry

$$L_{Ne} = \begin{cases} O^+ + \bar{e} \xrightarrow{k_{15}} O + h\nu & \text{slow (Neglect)} \\[6pt] O^+ + N_2 \xrightarrow{k_1} NO^+ + N & \text{fast} \\[6pt] NO^+ + e \xrightarrow{k_{14}} N + O & \text{moderate} \\[6pt] O^+ + O_2 \xrightarrow{k_2} O_2^+ + O & \text{fast} \\[6pt] O_2^+ + e \xrightarrow{k_{13}} O + O & \text{moderate} \end{cases}$$
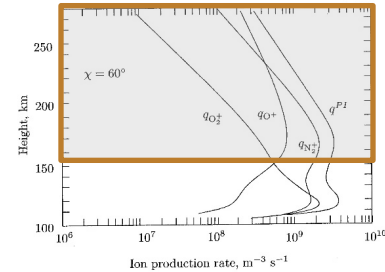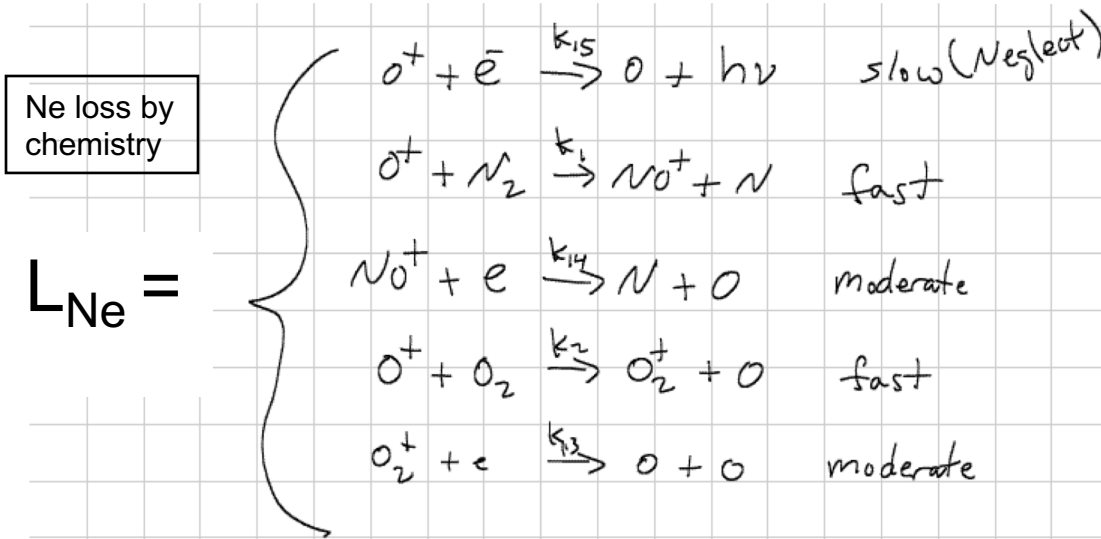
$$P_{O^+} = L_{O^+} \quad ==> \quad q(O^+) = (k_1[N_2] + k_2[O_2])[O^+]$$

F_2-Region Peak: A Balance of Chemistry and Transport
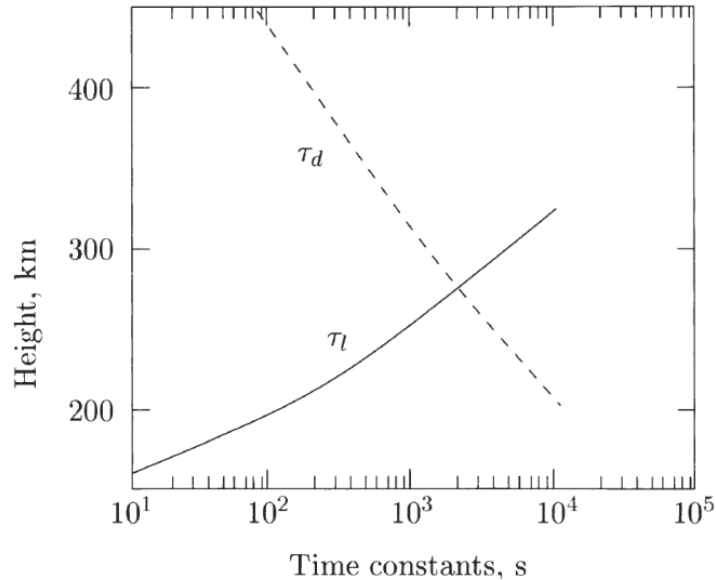
Diffusion time constant

$$t_d = \frac{H_p^2}{D_p} \qquad 2500 \sec @ 250km$$

Chemical time constant

$$t_l = \frac{1}{b} \qquad 2500 \sec @ 250km$$

In the F region, parallel transport (diffusion/vertical pressure gradients) can be as important as chemistry and both processes must be considered when assessing the electron density distribution.

n_i, ion number density for constituent i, $[m^{-3}]$

$n_i V_i$, number flux for constituent i, $[m^{-2}s^{-1}]$

P_i-L_i, production and loss rates of constituent i, $[m^{-3}s^{-1}]$

$(n_i V_i$ number flux parallel to B)

$$\frac{\partial n_i}{\partial t} = P_i - L_i - \nabla \sum (n_i V_i)$$

Equatorward wind at mid latitudes with inclined magnetic field pushes plasma upward along the magnetic field direction to regions of different neutral composition
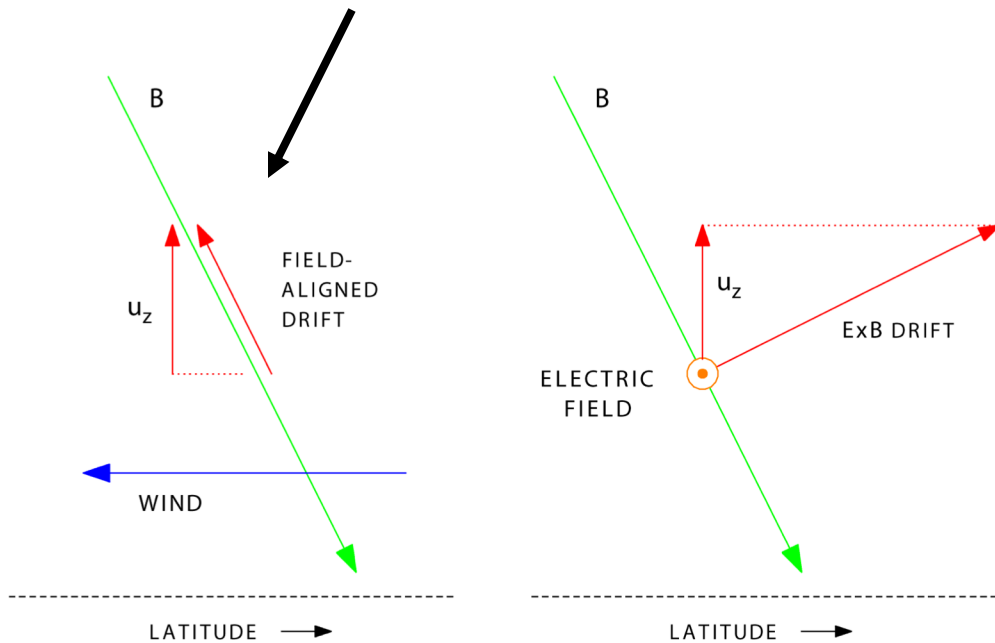
Wind effect on ionosphere at mid-latitudes with inclined magnetic field

- Equatorward wind pushes plasma upward in the direction of the geomagnetic field to regions of less molecular species N_2 and O_2, slowing loss rates, and driving a "positive phase" in the ionosphere
- Thermal expansion creates a vertical wind which can also push plasma along an inclined magnetic field to higher altitudes

Why NO⁺ in the E region

- [NO] is a minor species so there is little production by photoionization

- [NO⁺] is largely gained by charge exchange reactions (1), (6), and (7). Eventually the gain is offset by a loss to dissociative recombination (14) as the [NO⁺] concentration increases

- [N₂⁺] is lost through charge exchange reactions (4)-(6) that are faster than the loss due to dissociative recombination (12)

- Even though k4 is slower than k12, it is the much greater concentration of [O₂] to [Nₑ] that drives the loss rate

$$L(N2+) = k4[N2+][O2] \gg k12[N2+][Ne]$$

Ion Composition Profile
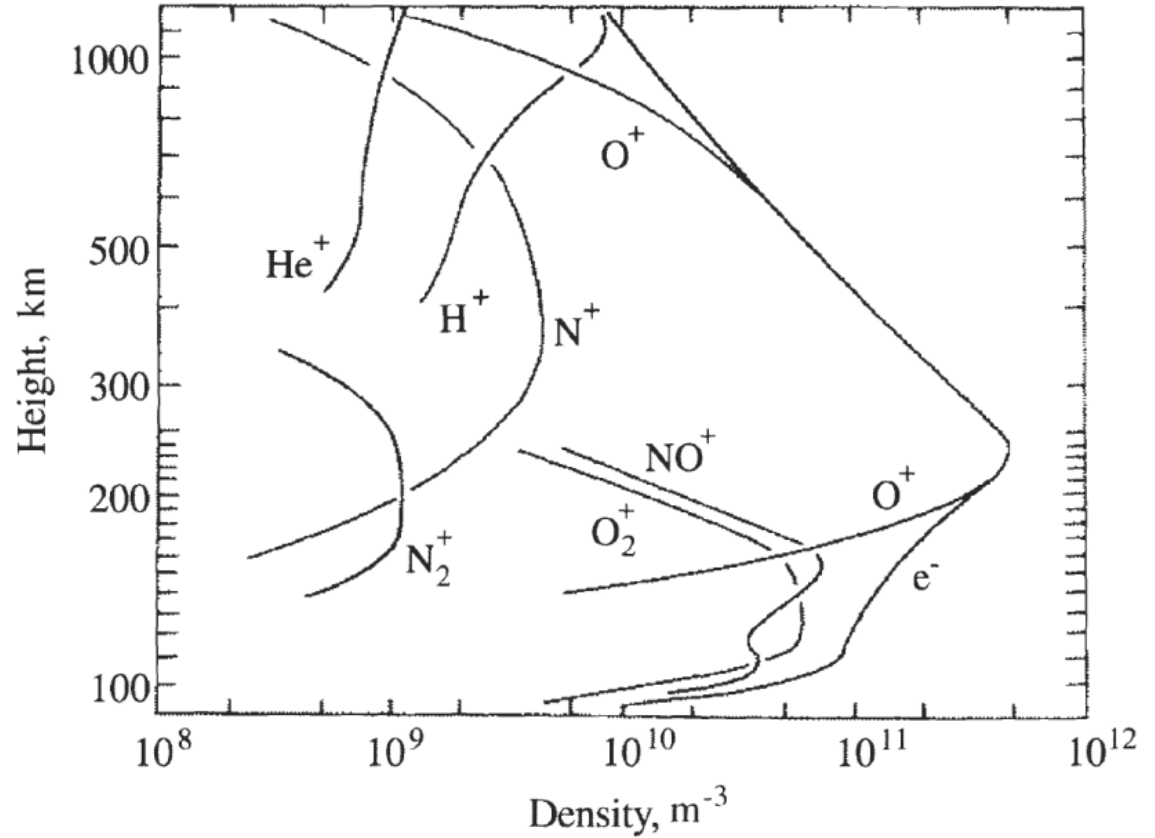
Fig. 4.2. The composition of the ionosphere as observed during the day at latitudes for low solar activity (adapted from Johnson, 1966)

July 16th, 2020

27

Ion motion – Forces on plasma

- Coulomb force - e **E**

- Ion in motion: Lorentz force - e **VxB**

- Collisions with neutrals - $m\upsilon(V\text{-}U)$

- Gravity

- Mobility parallel to B is high, and perpendicular to B is low

Perpendicular Plasma Motion with Neutral Winds

$$n_i m_i \frac{dV_i^\perp}{dt} = en_i\left(\vec{E}^\perp + \vec{V}_i^\perp \times \vec{B}\right) - n_i m_i \upsilon_{in}\left(\vec{V}_i^\perp - \vec{U}_n^\perp\right)$$

$$n_e m_e \frac{dV_e^\perp}{dt} = en_e\left(\vec{E}^\perp + \vec{V}_e^\perp \times \vec{B}\right) - n_e m_e \upsilon_{en}\left(\vec{V}_e^\perp - \vec{U}_n^\perp\right)$$

Ion momentum equation

$$\vec{V}_i' = \vec{V}_i - \vec{U}_n = \frac{1}{1+k_i^2}\left\{\frac{k_i}{B}\vec{E}' + \left(\frac{k_i}{B}\right)^2 \vec{E}' \times \vec{B} + \left(\frac{k_i}{B}\right)^3 \left(\vec{E}' \bullet \vec{B}\right)\vec{B}\right\}$$

$$\vec{E}' = \vec{E} + \vec{U}_n \times \vec{B}$$

Electron momentum equation

$$\vec{V}_e' = \vec{V}_e - \vec{U}_n = \frac{1}{1+k_e^2}\left\{\frac{-k_e}{B}\vec{E}' + \left(\frac{k_e}{B}\right)^2 \vec{E}' \times \vec{B} - \left(\frac{k_e}{B}\right)^3 \left(\vec{E}' \bullet \vec{B}\right)\vec{B}\right\}$$

Height dependence of ion motion perpendicular to B

$$\Omega/\upsilon_{in} < 1 \qquad \vec{V}_i^{\perp} \approx \vec{F}^{\perp}$$

$$\Omega/\upsilon_{in} > 1 \qquad \vec{V}_i^{\perp} \approx \upsilon_{in}/\Omega \, \vec{F} \times \hat{b}$$

$$\vec{V} = \frac{e}{m\upsilon} \vec{E}$$

Ion Motion

$$\vec{V} = \frac{\vec{E} \times \vec{B}}{B^2}$$

60 80 100 130 160 200 240 300

Electron Motion

$$\vec{V} = \vec{U}$$

Ion Motion

$$\vec{V} = \frac{\upsilon}{\Omega} \vec{U} \times \hat{b}$$

60 80 100 130 160 200 240 300

Electron Motion

Heliophysics Summer School I-T

Neutral Dynamics in pressure coordinates

$$\frac{\partial}{\partial t} V_\theta = -\frac{V_\theta}{r}\frac{\partial}{\partial \theta} V_\theta - \frac{V_\phi}{r\sin\theta}\frac{\partial}{\partial \phi} V_\theta - \omega\frac{\partial}{\partial p} V_\theta - \frac{g}{r}\frac{\partial}{\partial \theta} h +$$

horizontal and vertical advection   pressure

$$\left(2\Omega + \frac{V_\phi}{r\sin\theta}\right) V_\phi \cos\theta + g\frac{\partial}{\partial p}\left[(\mu_m + \mu_T)\frac{p}{H}\frac{\partial}{\partial p} V_\theta\right] - \nu_{ni}\left(V_\theta - U_\theta\right)$$

(13)

Coriolis and "curvature"   vertical viscosity   ion drag

and

$$\frac{\partial}{\partial t} V_\phi = -\frac{V_\theta}{r}\frac{\partial}{\partial \theta} V_\phi - \frac{V_\phi}{r\sin\theta}\frac{\partial}{\partial \phi} V_\phi - \omega\frac{\partial}{\partial p} V_\phi - \frac{g}{r\sin\theta}\frac{\partial}{\partial \phi} h -$$

$$\left(2\Omega + \frac{V_\phi}{r\sin\theta}\right) V_\theta \cos\theta + g\frac{\partial}{\partial p}\left[(\mu_m + \mu_T)\frac{p}{H}\frac{\partial}{\partial p} V_\phi\right] - \nu_{ni}\left(V_\phi - U_\phi\right)$$

(14)

Quiz

- Which region of the solar atmosphere is most like the thermosphere?

- Photosphere, chromosphere, or corona?

Break

Heliophysics Summer School I-T

Similarities between the chromosphere and the thermosphere/ionosphere

- Partially ionized plasma, mostly gravitationally bound

- Not chaotic in their own right

- Strongly driven by underlying chaotic (or non-stationary) convective atmospheres: photosphere and troposphere

- Overlain by a strongly ionized and magnetized plasma: corona and magnetosphere

- Strong ion-neutral coupling

- Collision dominated - transition from collisional to collision-less near upper layers

- Plasma instabilities, e.g., Rayleigh-Taylor

Chromosphere / Ionosphere Comparison
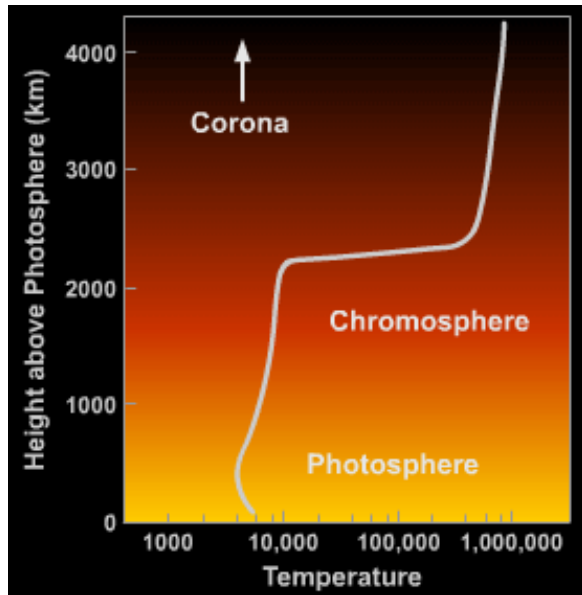
Solar Chromosphere
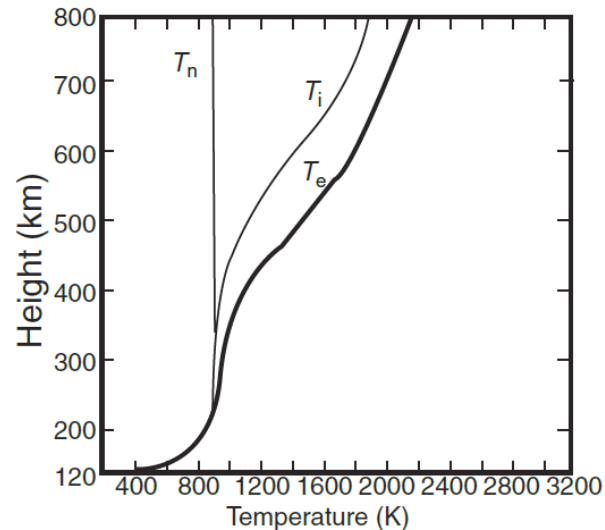
Earth's Ionosphere/Thermosphere

Heliophysics Summer School I-T

Differences between the chromosphere and the thermosphere/ionosphere

- Temperature, ion fraction and conductivity

- Magnetic field changes [0.01 (1%) vs 100]

- Ionization from heat vs ionization from EUV

- Ions a much stronger driver of the system

- Treated as a **B**, **V** system vs a **J**, **E** system

- T-I also driven from above

- Fully turbulent vs transition to molecular separation

Excellent review by: Leake et al., Ionized Plasma and Neutral Gas Coupling in the Sun's Chromosphere and Earth's Ionosphere/Thermosphere, Space Sci. Rev., Doi:10.1007/s11214-014-0103-1, 2014.

Coupled Thermosphere Ionosphere Plasmasphere Electrodynamics Model (CTIPe)

• Global thermosphere 80 - 500 km, solves momentum, energy, composition, etc. Vx, Vy, Vz, Tn, O, O2, N2, … Neutral winds, temperatures and compositions are solved self consistently with the ionosphere (Fuller-Rowell and Rees, 1980);

• High latitude ionosphere 80 -10,000 km, solves continuity, momentum, energy, etc. O^+, H^+, O_2^+, NO^+, N_2^+, N^+, V_i, T_i, …. (open flux tubes) (Quegan et al., 1982;

• Plasmasphere, and mid and low latitude ionosphere, closed flux tubes to allow for plasma to be transported between hemispheres (Millward et al., 1996) ;

• Self-consistent electrodynamics (electrodynamics at mid and low latitudes is solved using conductivities from the ionospheric model and neutral winds from the neutral atmosphere code) (Richmond et al.,);

• Forcing: solar UV and EUV, Weimer electric field, TIROS/NOAA auroral precipitation,WAM tidal forcing.

CTIPe model - global thermosphere-ionosphere fields

00UT

Temperature

Height-integrated O/N$_2$ ratio

Meridional wind

Ne

July 16th, 2020
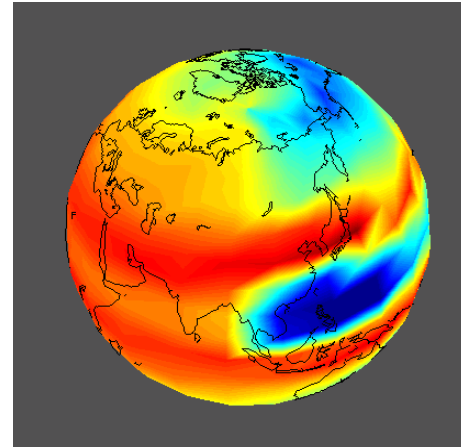
Impact of Ion Drag/Viscosity

- Zonal winds damped by drag (ion-drag or viscosity)

- Meridional pressure gradient no longer balanced Coriolis force on zonal wind

- Zonal mean meridional wind develops

- Global composition structure develops

- Semi-annual variation present

- Global structure not only dependent on magnitude of pressure gradient but also dependent on magnitude of zonal drag.
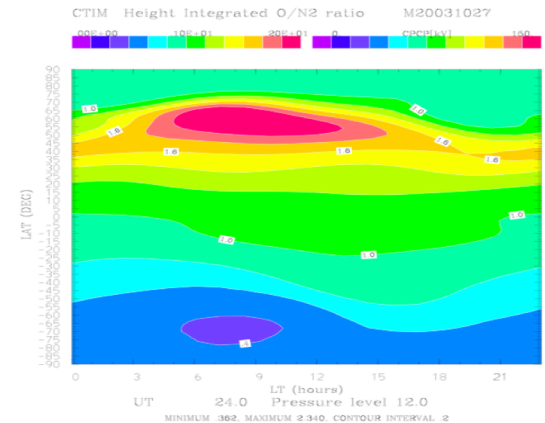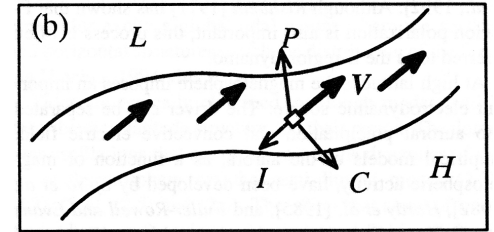
Neutral Composition and Global Circulation

upwelling reduces O/N_2 (increase mean mass)
downwelling increases O/N_2 (decrease mean mass)
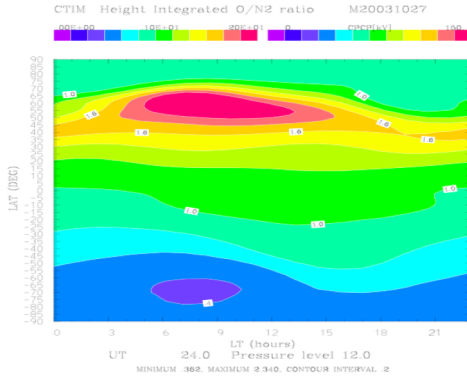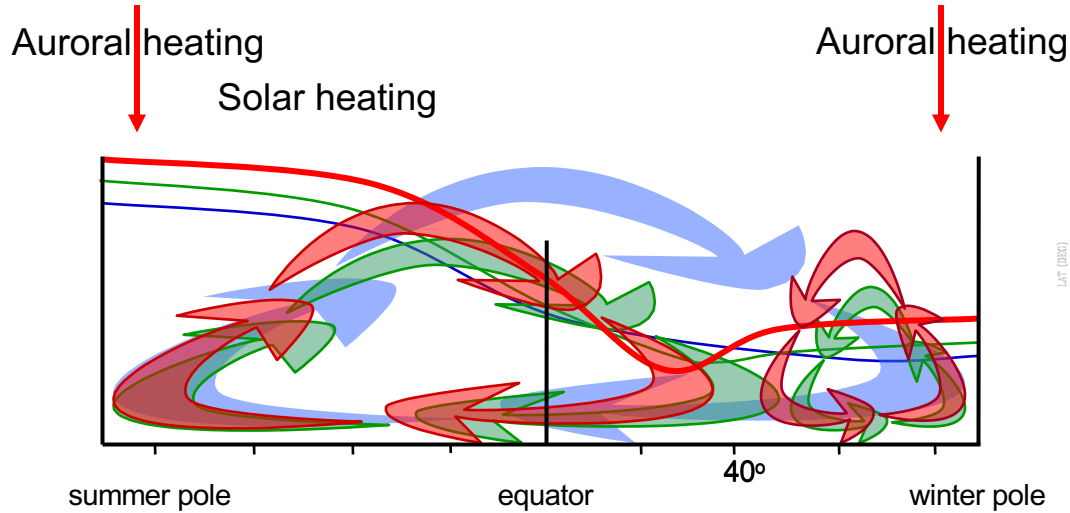
Araujo-Pradere et al

——— solar driven circulation, quiet conditions (kp = 0)

——— quiet conditions (kp = 2+)

——— perturbed conditions (kp = 7)

Sources of vertical wind and composition change

$$\frac{\partial \omega}{\partial p} = -\nabla_p \cdot \overline{V}$$

$$V_z = \left(\frac{\partial h}{\partial t}\right)_p - \frac{\omega}{\rho g}$$

•Thermal expansion causes a change in composition on fixed height but no change on constant pressure levels
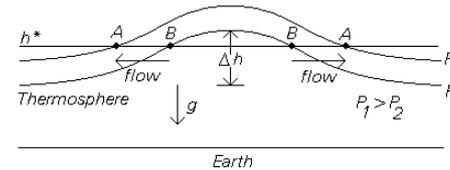
•Localized thermal expansion generates horizontal pressure gradients and a divergent wind field and upwelling through pressure levels
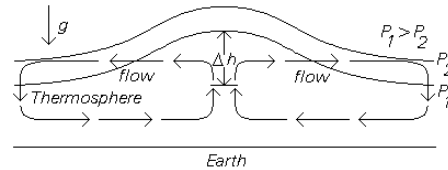
$$\frac{\partial \psi_i}{\partial t} = \frac{1}{\rho} m_i S_i - \overline{V} \cdot \nabla p \psi_i - \omega \frac{\partial}{\partial p} \psi_i - \frac{1}{\rho} \nabla \cdot (n_i m_i C_i) + \frac{1}{\rho} \nabla (K_T n_i \nabla m_i \psi_i)$$

A few basics on neutral composition change

- Hydrostatic equilibrium is not the same as diffusive equilibrium

- Heating the gas and thermal expansion change the ratio of neutral species (O/N_2) on height levels

- Heating and thermal expansion does not change the ratio of neutral species (O/N_2) on pressure surfaces

- Pressure surfaces are important because they represent layers of constant optical depth or level of deposition of an ionizing photon or electron

- "Real" changes in neutral composition is caused by upwelling through pressure surfaces, which is driven by divergence of horizontal winds

- Gravitationally bound, close to hydrostatic balance

- Collision dominated up to ~600 km - transition from collisional to collision-less near upper layers

- Fluid (gas laws, temperature T, pressure p, number density n, mass density ρ, $p = nkT$, Navier-Stokes equations)

- Heated, ionized, and dissociated by solar EUV/UV radiation and aurora (photo-chemistry, Chapman profiles)

- Partially ionized plasma < 1% (100-600km altitude)

- Not chaotic in its own right

- Strongly driven by underlying chaotic (or non-stationary) convective atmosphere: troposphere

- Overlain by a strongly ionized and magnetized plasma: magnetosphere

- Sits in Earth's magnetic field 22,000 to 67,000 nT - 99% invariant on short timescales $\Delta B \sim 1000$ nT

- Strong ion-neutral coupling

- Plasma instabilities, e.g., Rayleigh-Taylor

Thermosphere/ Ionosphere)

Ionospheric Electric Potential   06/18/95   6.7 UT
IMF B_Y= -1.9 nT B_Z= -7.9 nT   SW Vel= 350.0 km/sec
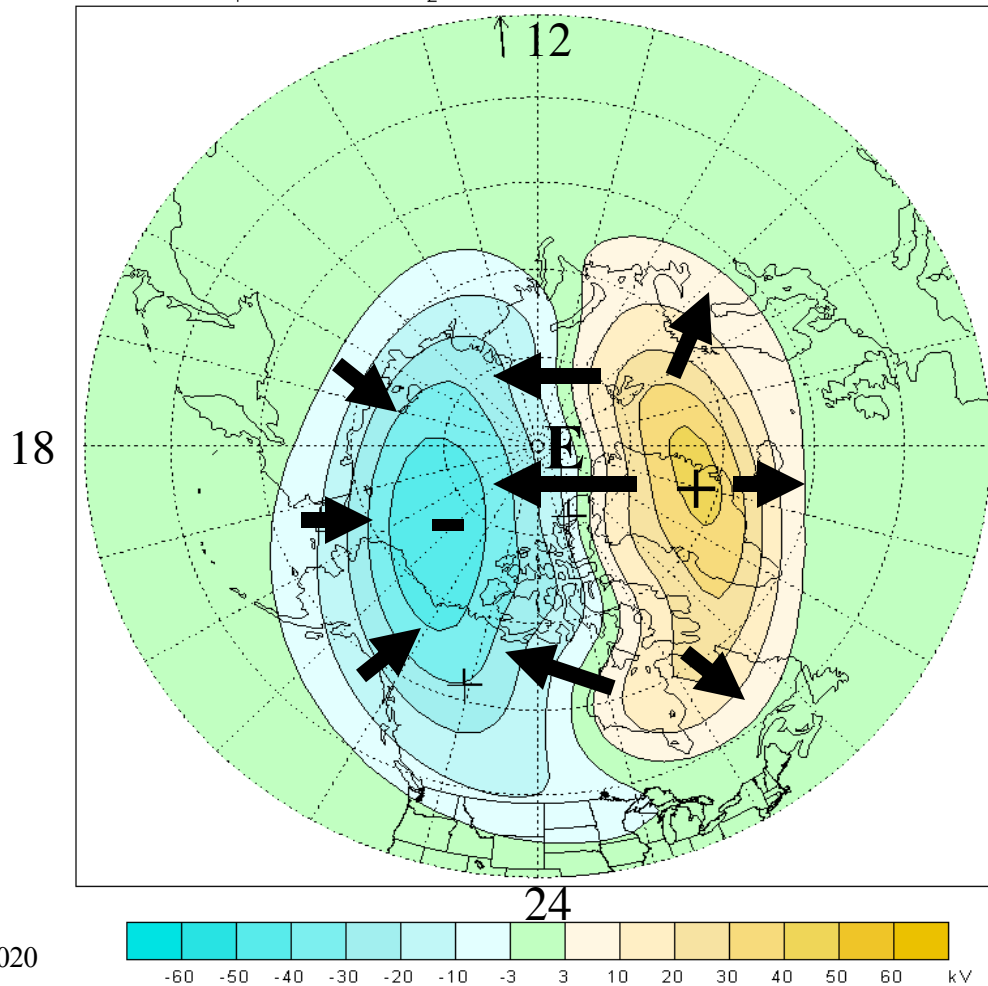
Ion drift:
Above ~160 km **ExB**
Below 160 km as collision with neutral atmosphere become more important ion drift rotates towards the **E**-field vector and reduces in magnitude
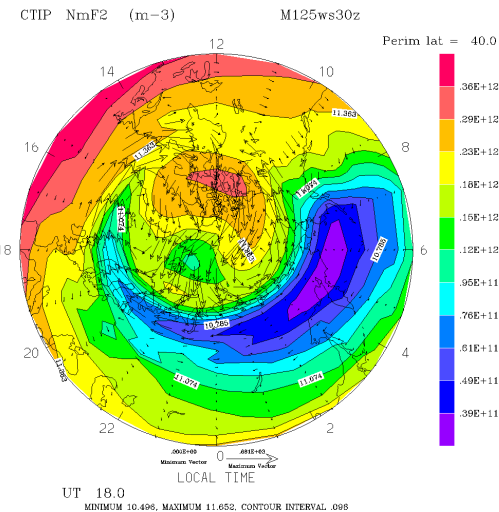
July 16th, 2020

44

Ion-neutral collisions in upper thermosphere frequent enough to drive high velocity neutral wind

Neutral Winds and Temperature: 300 km altitude
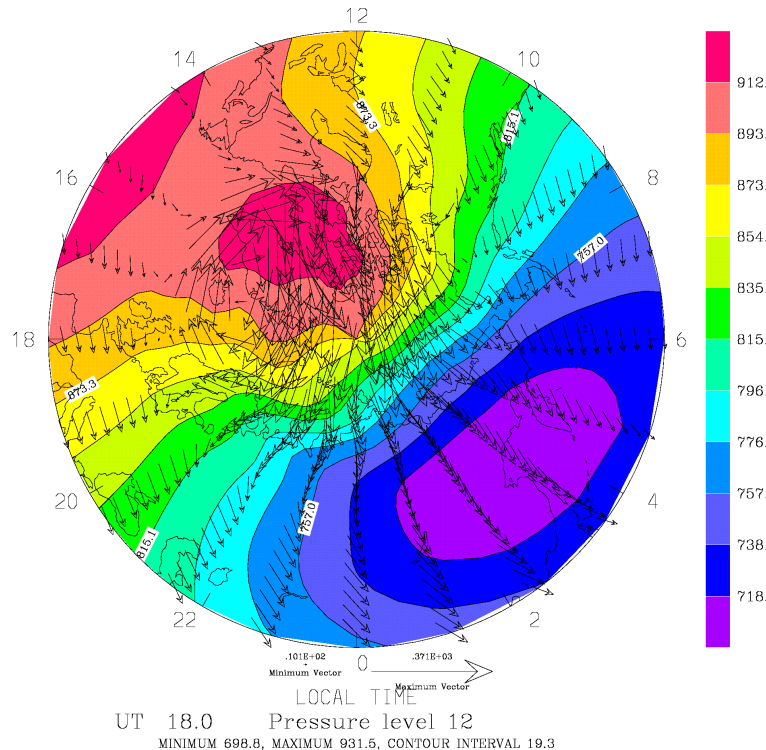
Maximum wind speed observed by DE-2 satellite ~ 1400 m/s

ExB ion drift and NmF2
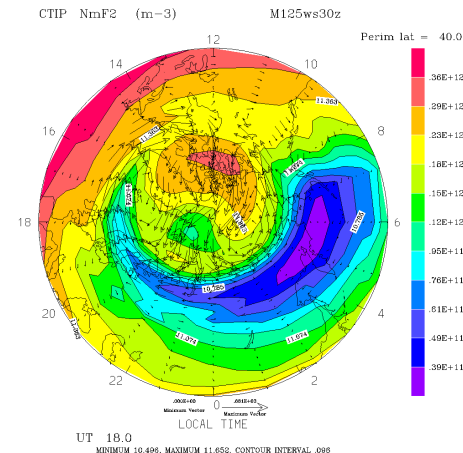
In-track wind of 1400 m/s changes "apparent" density by 35% for LEO moving at 8 km/s

Ion-neutral collisions in upper thermosphere frequent enough to drive high velocity neutral wind

Neutral Winds and Temperature: 300 km altitude
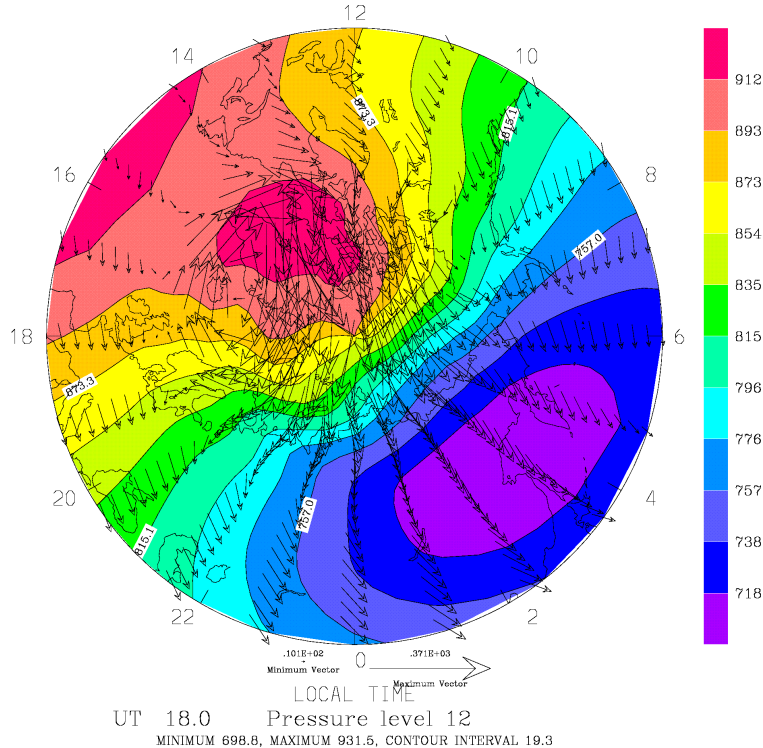
Maximum wind speed observed by DE-2 satellite ~ 1400 m/s (3683 mph!) Cat. 5 Hurricane >155 mph

ExB ion drift and NmF2
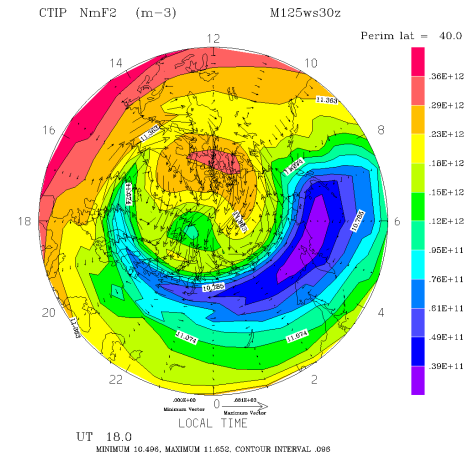
In-track wind of 1400 m/s changes "apparent" density by 35% for LEO moving at 8 km/s

Non-linear effects

- Compare with hurricane speeds:
  150 mph ≡ 60 m/s
  1500 mph ≡ 600 m/s
- Transport/advection and acceleration strong
- Asymmetry in response in dawn and dusk sectors
- Inertial motion on a non-rotating sphere is a great circle
- Spherical co-ords e.g. east/west, is not cartesian system
- Introduces "curvature" terms
- Inertial oscillation

July 16th, 2020   Heliophysics Summer School I-T
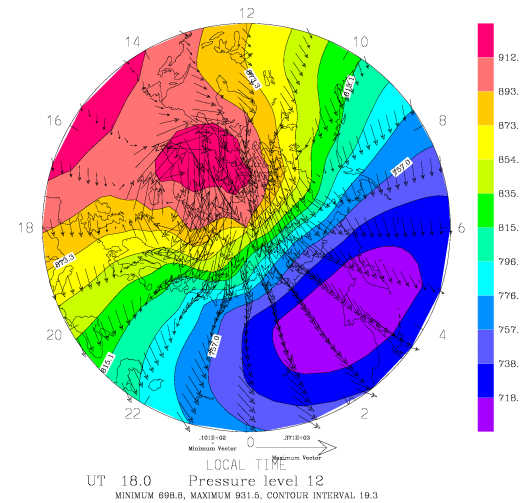
Inertial Oscillation:
balance between centrifugal (curvature) and Coriolis

Ion-drag

$\mathbf{V}$

Curvature
V^2/R
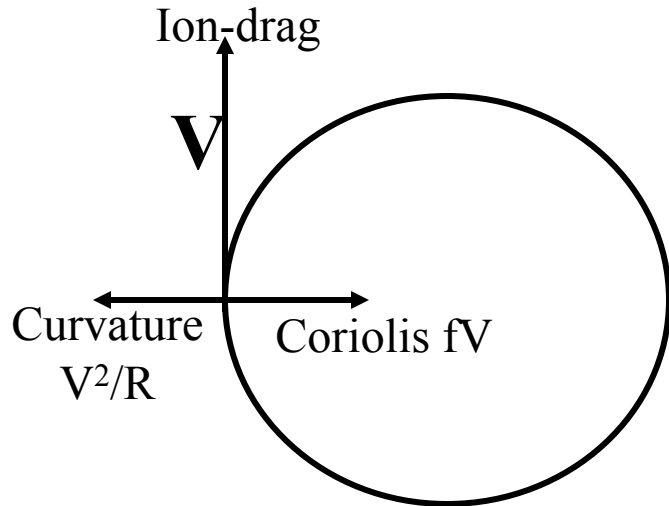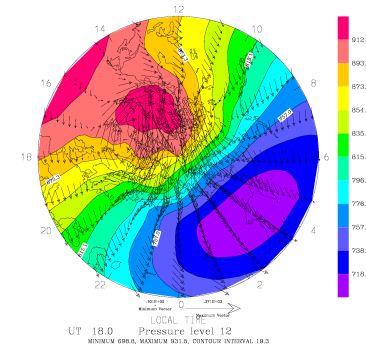
Coriolis fV

$$\frac{V^2}{R} = -fV$$

Radius of curvature R=20° latitude
Coriolis high latitude f=1.4x10^{-4}
V~300m/s, convergent if slower,
divergent if stronger

Inertial Resonance

Ionospheric Electric Potential 06/18/95 6.7 UT
IMF B_y= -1.9 nT B_z= -1.9 nT SW Vel= 350.0 km/sec

- Coriolis force directs winds towards the right in the northern hemisphere

- Tends to move parcels of gas in clockwise vortex, similar to dusk plasma convection cell

- In dusk sector Coriolis tends to constrain parcels within curvature of auroral oval

- In dawn sector gas tends to be expelled equatorward

- Gas constrained within auroral oval can be accelerated to high velocities

- Dawn sector momentum spread over wider area.
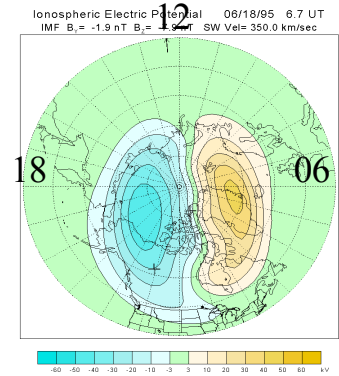
Dawn Cell:
centrifugal (curvature) and Coriolis assist
$\Rightarrow$ low pressure cell

Ion-drag

V

Coriolis fV

L

Curvature
V²/R
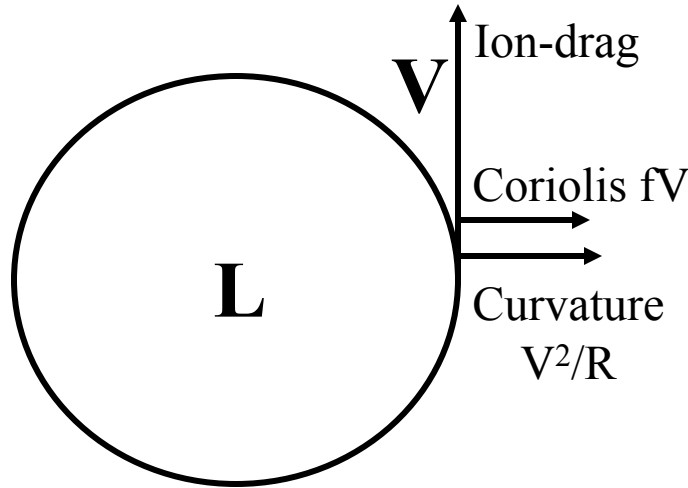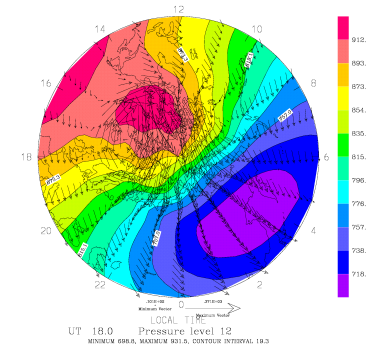
$$\frac{V^2}{R} + fV = -\frac{1}{\rho}\frac{\partial p}{\partial n}$$

Vortex in dawn cell always
divergent if ion-drag forcing
is cyclonic (anti-clockwise)

Storm-time neutral winds produce dynamically driven "holes"

Dawn cell always divergent - typically see density hole
Dusk cell only divergent when wind
speeds exceed 300 or 400 m/s

CTIP NEUTRAL TEMPERATURE (DEG. K) M125eqst3

LOCAL TIME

UT 18.0 Values at 200.0 [km]
MINIMUM 709.6, MAXIMUM 1001.0, CONTOUR INTERVAL 24.2

CTIP Total Mass Density (kg m-3) M125eqst3

LOCAL TIME

UT 18.0 Values at 200.0 [km]
MINIMUM 2.016×10⁻¹⁰, MAXIMUM 3.775×10⁻¹⁰, CONTOUR INTERVAL 0.146×10⁻¹⁰
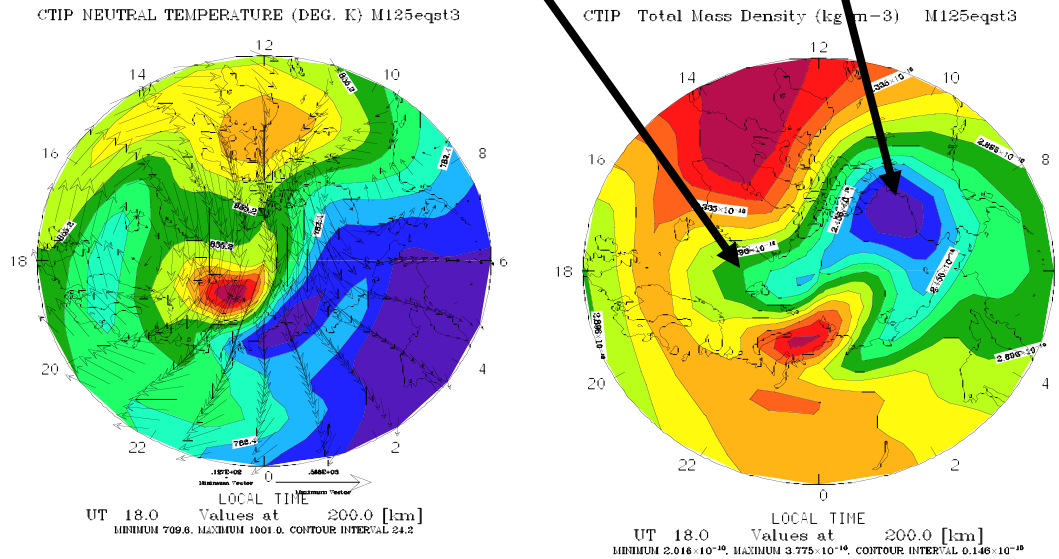
Structure and variability of vertical wind, temperature, and density at 250 km altitude in response to waves from lower atmosphere

Model Layer 128 Temperature at 03/17/13 00:00Z

250km W at 2013/03/16 03Z
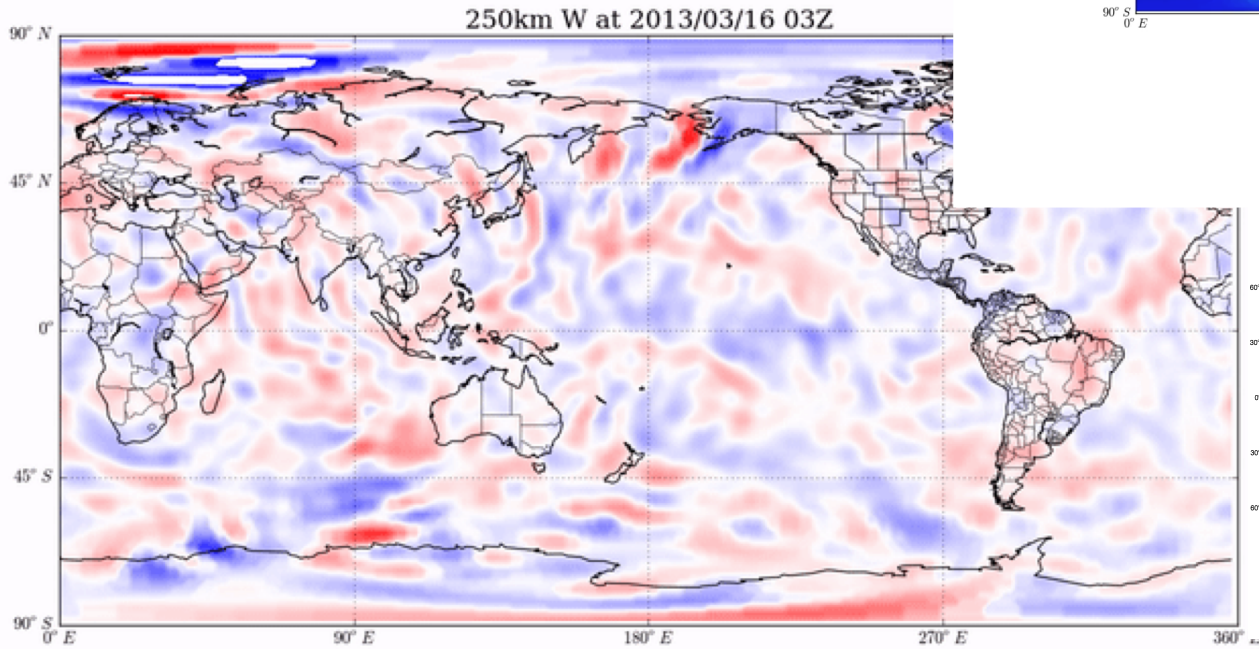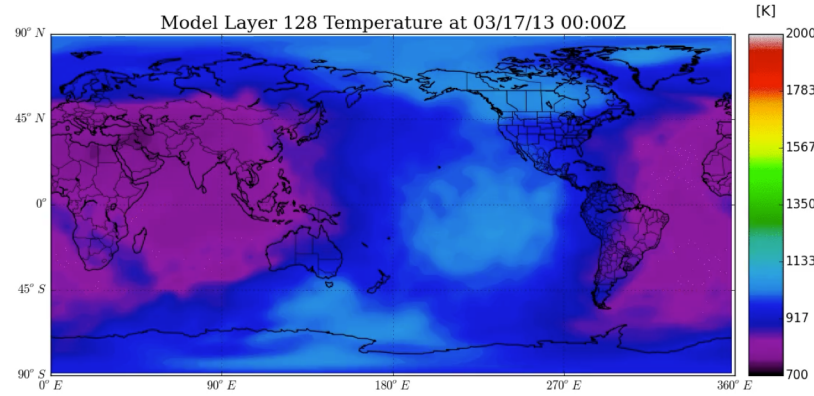
Neutral temperature (above)
neutral density (below)
250km altitude

WAM Global Neutral Mass Density at   240.000km and GOCE at   236.15142 km on March 16 at   1.00000UT Hours
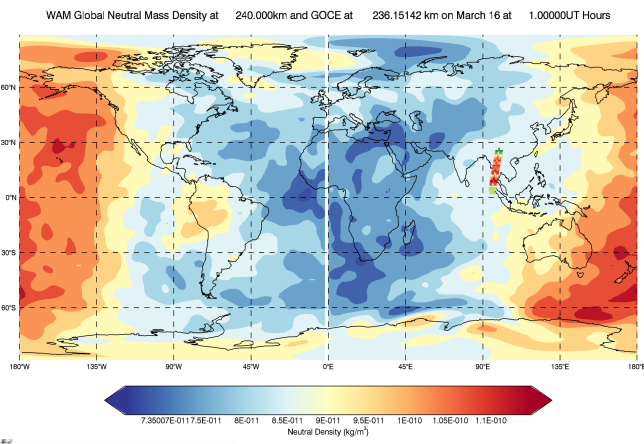
Four peak longitude structures in the ionosphere
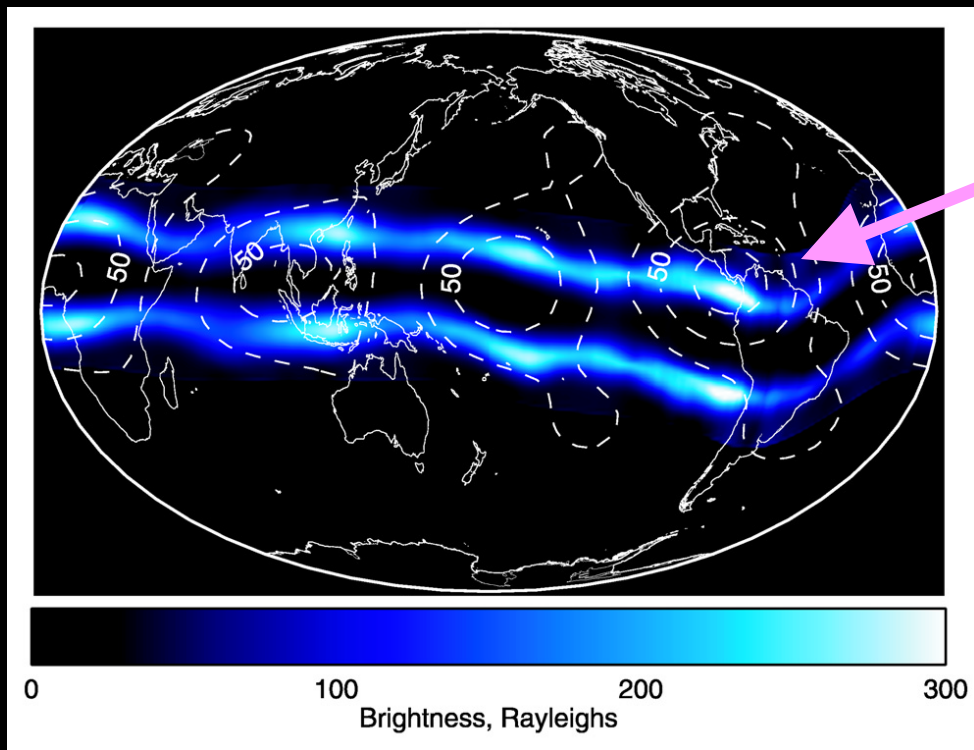
IMAGE composite of 135.6-nm O airglow (350–400 km) in March–April 2002 for 20:00 LT and amplitude of modeled diurnal temperature oscillation @ 115 km (Immel et al., 2006).

The four peaks driven by nonmigrating eastward propagating tidal mode with zonal wavenumber 3 (DE3) in dynamo region.
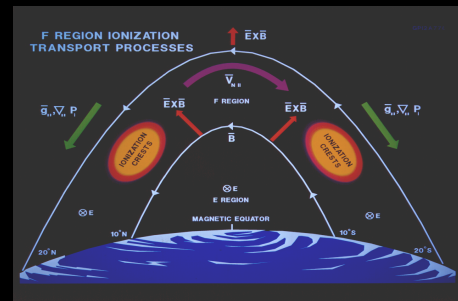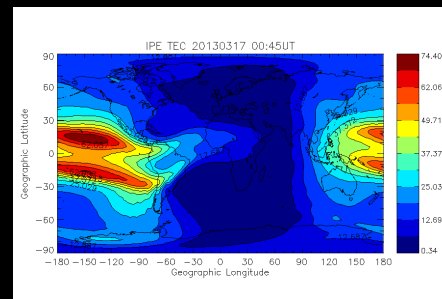
Driver of the Immel longitude structure

90°
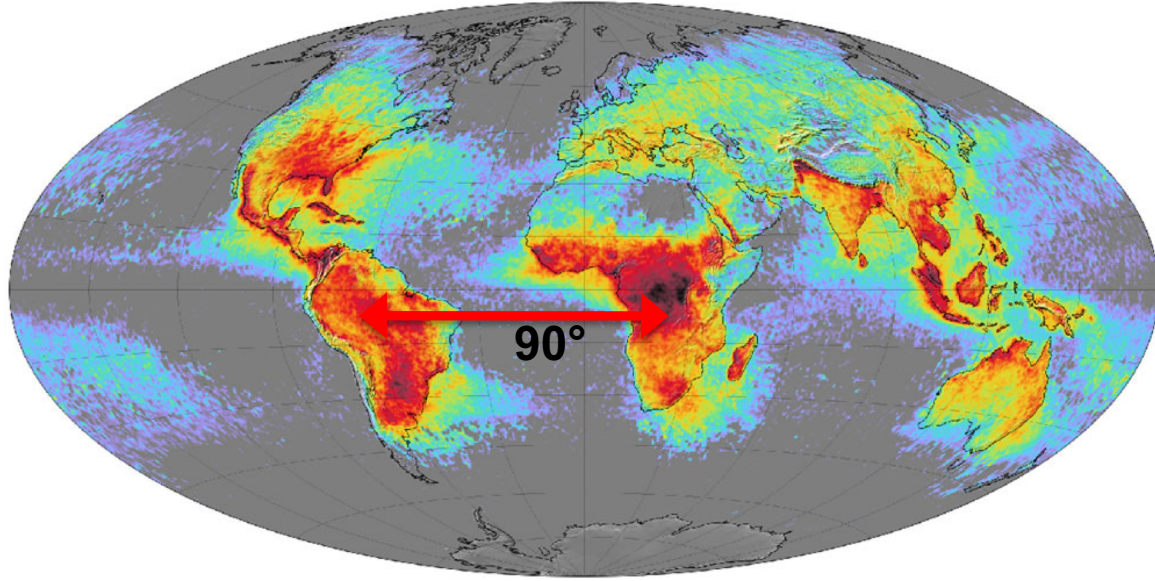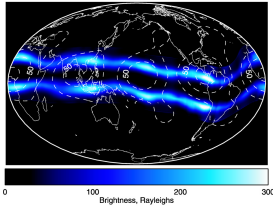
Lightning strikes from convective storms, signature of latent heat release:
Either three or four peaks in longitude: wave 3 or 4
Illuminated by the Sun every 24 hours: diurnal

$$\cos(\Omega t + \lambda) \cos 4\lambda \quad \text{---}> \quad \cos(\Omega t + 5\lambda) + \cos(\Omega t - 3\lambda)$$

$$\cos(\Omega t + \lambda) \cos 3\lambda \quad \text{---}> \quad \cos(\Omega t + 4\lambda) + \cos(\Omega t - 2\lambda)$$

Can create a diurnal eastward propagating W2 or W3 DE2 and DE3

50% increase in TEC in January 2009 when solar and geomagnetic activity were very low

Goncharenko et al. 2010
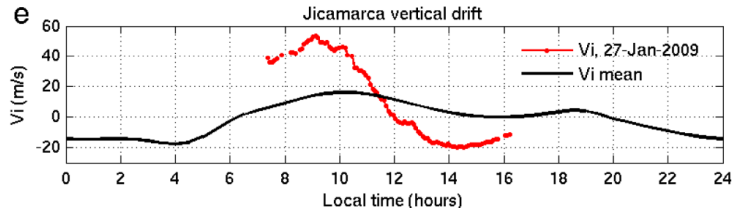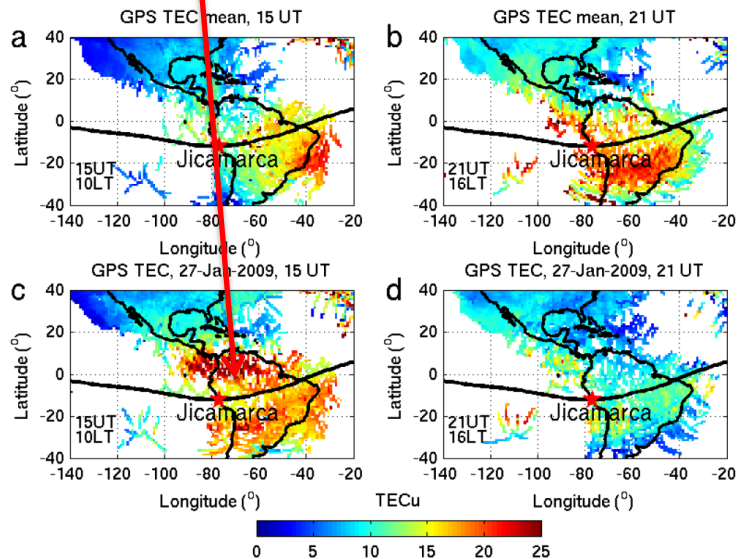
Is this also a response to changing tidal amplitudes?
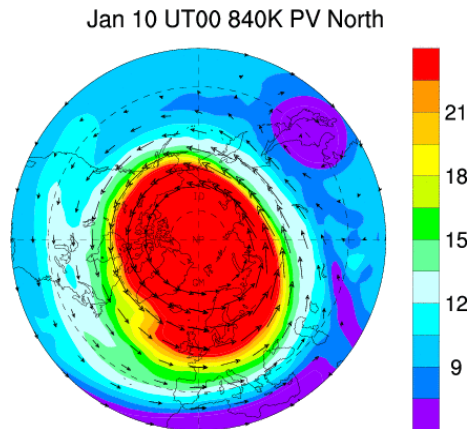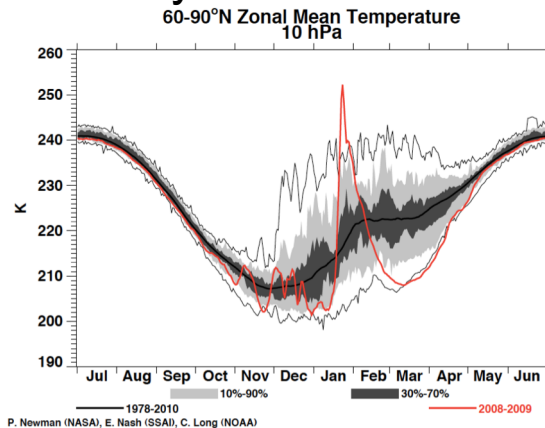
Sudden stratospheric warming

Benefits of WAM

- Compatible with the US weather model already running operationally
- Can implement the operational Gridpoint Statistical Interpolation (GSI) data assimilation system, utilizing the lower atmosphere data
- Able to follow real lower atmosphere weather events and their impact on the upper atmosphere and ionosphere (such as hurricanes, tornados, planetary waves, sudden stratospheric warming, tropical convection, longitude structure in migrating and non-migrating tides)

WAM simulations of the January 2009 sudden stratospheric warming

60N 10hPa

90N 10hPa

70K

(b) JRO ΔVz (m/s)(2009)

kp <= 2
kp > 2

From: 8-Jan-2009 (8) to: 1-Mar-2009 (60)

Jan 10 UT00 840K PV North

60N 10hPa

CTIP+WAM ΔVz (m/s)

From Jan-11 to Feb-22

(a) NH
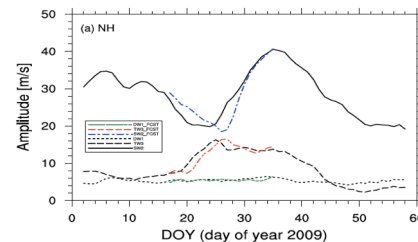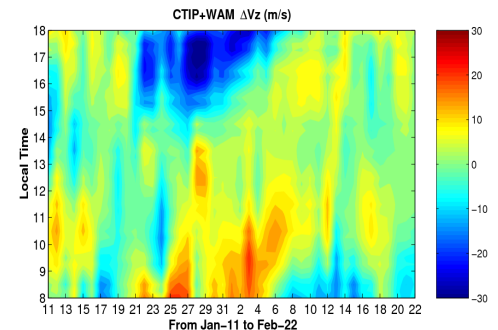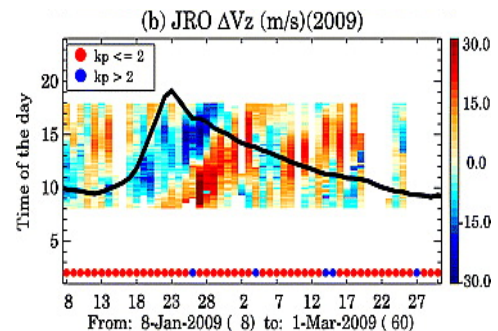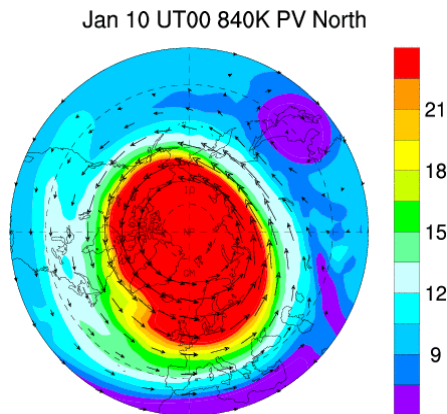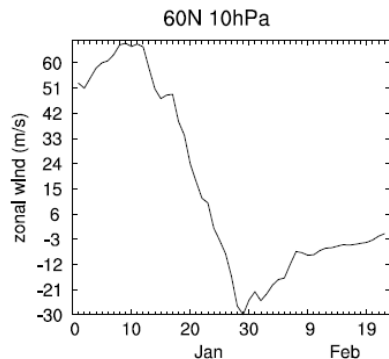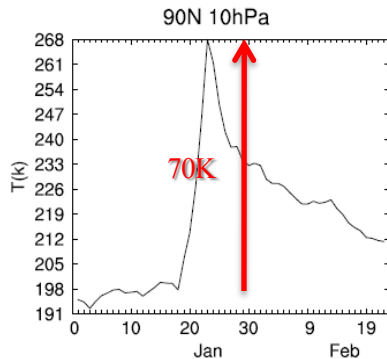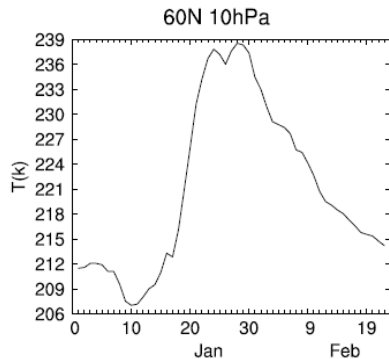
January 2009 Stratospheric Warming impact on EIA

GPS-TEC observation
before and after SSW
Goncharenko et al. (2010)

WAM-GIP
before and after SSW
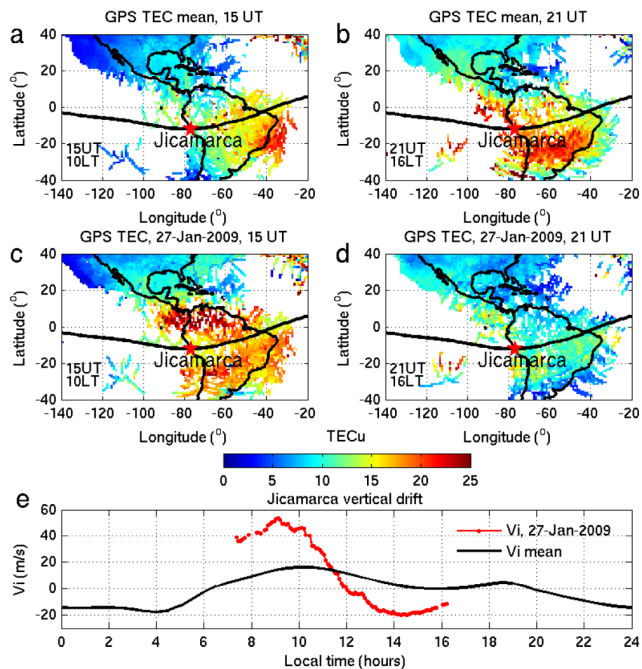
SSW vertical plasma drift
Jicamarca (Chau et al., 2010)
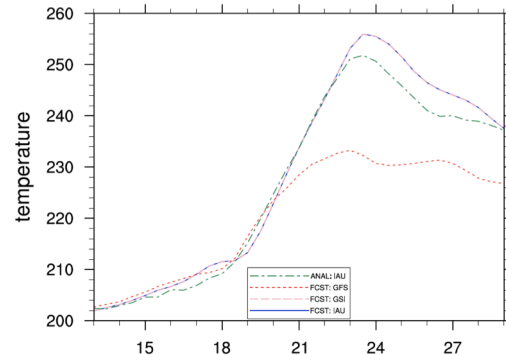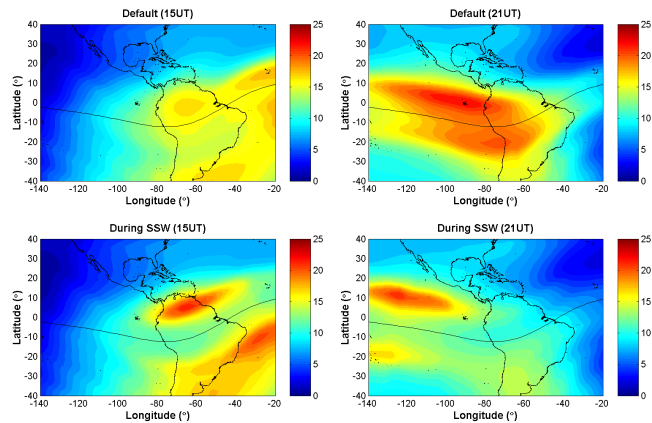
Can be forecast more than a week ahead

Midnight Temperature Maximum

- A previously unexplained secondary temperature maximum near midnight
- Appears to be the nightside branch of one of the peaks in ter-diurnal, westward propagating, wave number 3 (TW3)

Mar 20N UT00 285km

Model Layer 128 Temperature at 03/16/13 00:00Z

Dec 30S ΔT/T(%) UT12

December 30S UT12 waves 3-12

Dec 04 00:00 UT ΔT/T₀ (%) 30°N
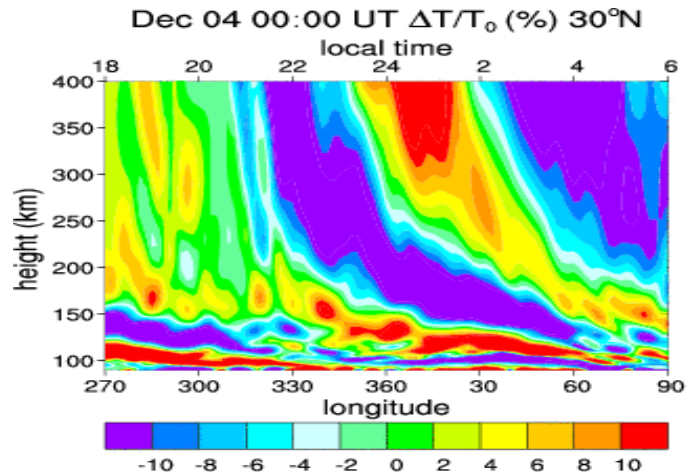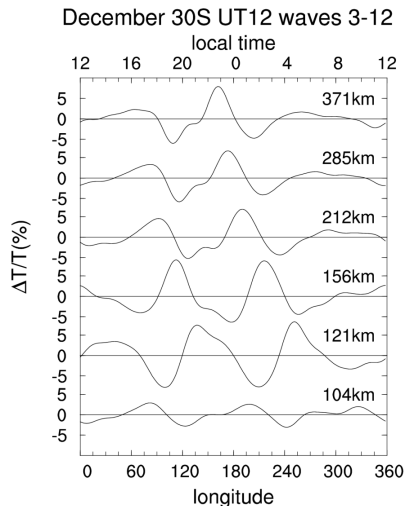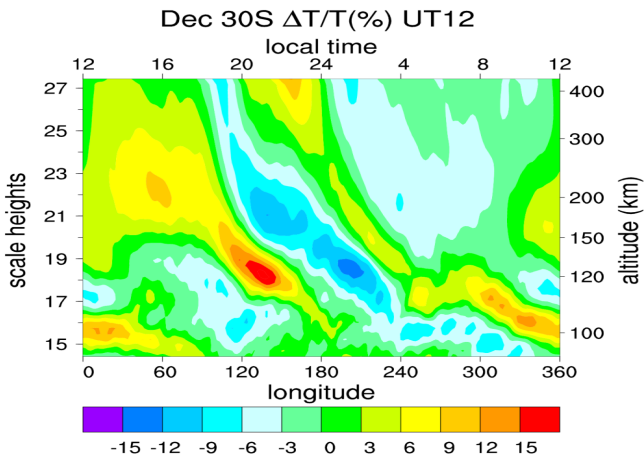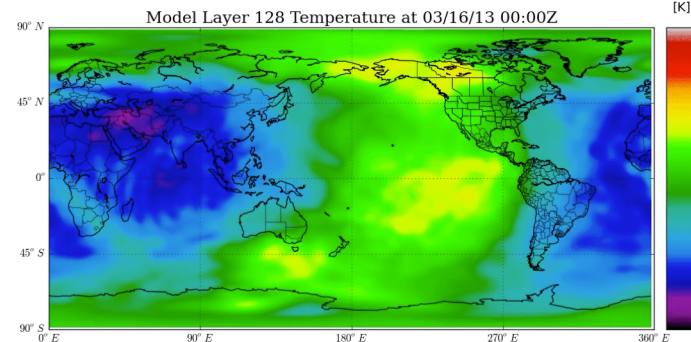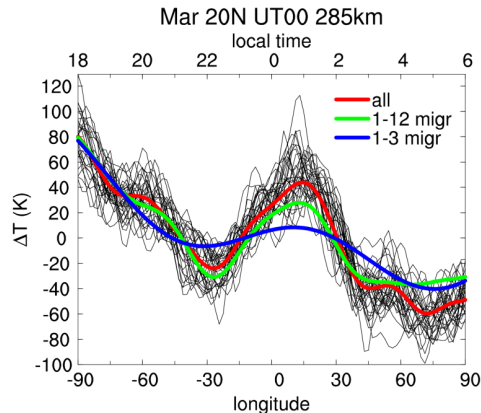
Use WAM winds, composition, density to drive GIP plasma density
- agrees well with Arecibo ISR observations by Djuth et al. -

WAM temperature perturbations at Arecibo
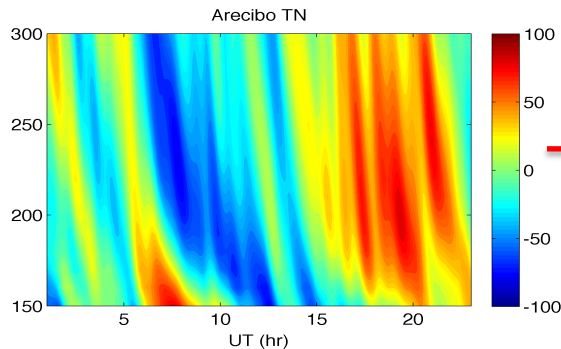
WAM-GIP ~20% plasma density perturbations at Arecibo
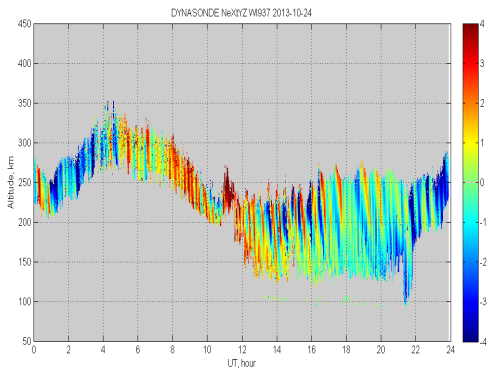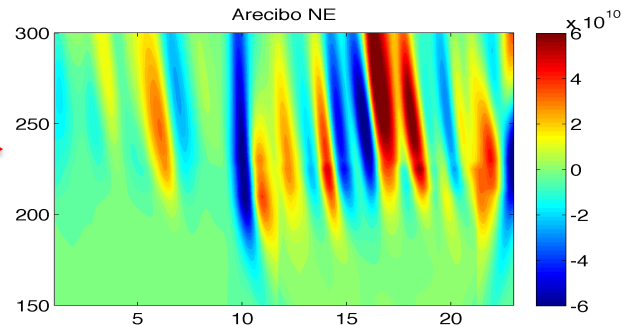
Dynasonde - vertical velocity and tilts, Nikolay Zabotin
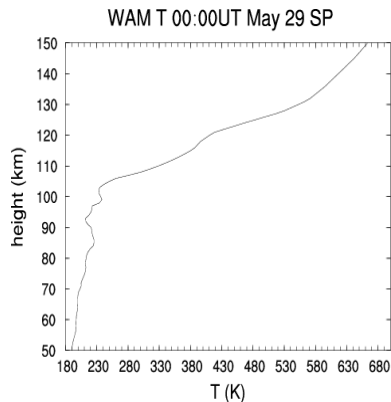
WAM temperature
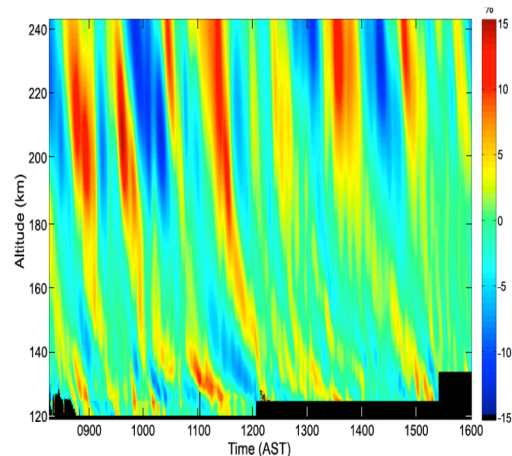
De-trended ISR observations of N_e perturbations, Djuth et al.

Bubble development in physics-based irregularity model (PBMOD) with WAM fields (180 km horizontal. resolution, ¼ scale-height vertical, ~2-5km) with no additional seeding Retterer et al.
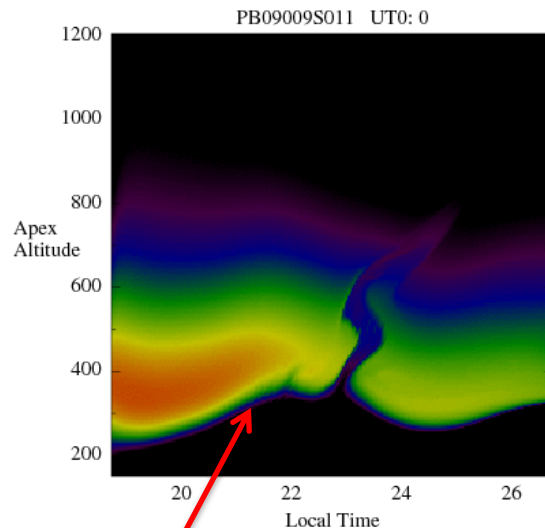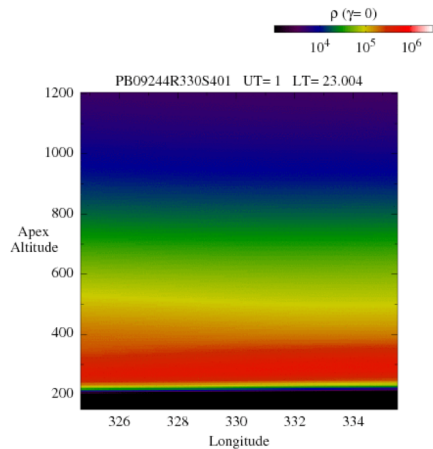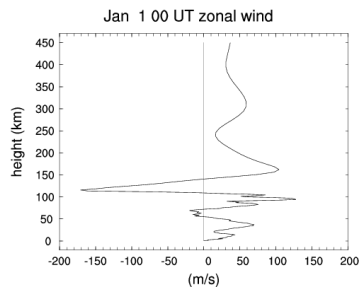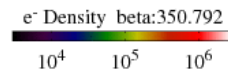
forecasting large scale wave structure, (LSWS) on bottomside
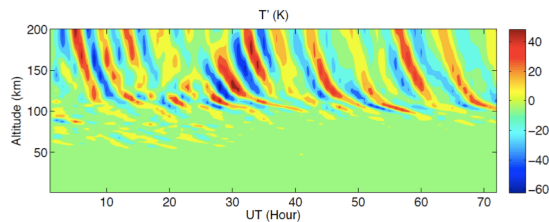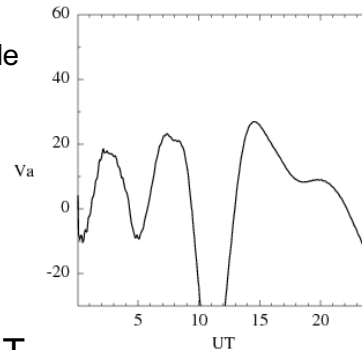
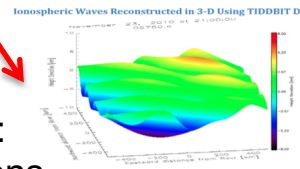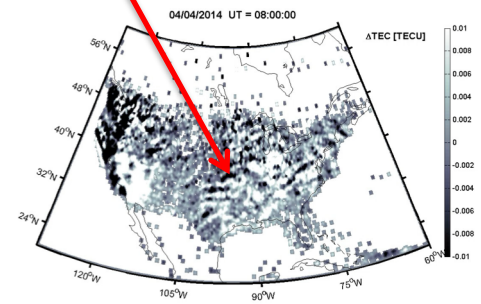# Waves propagate from tropospheric sources through the atmosphere
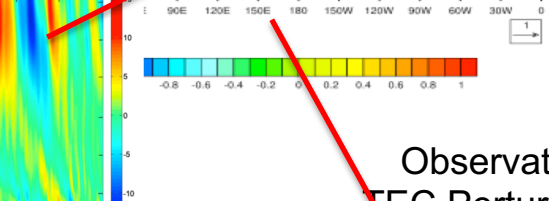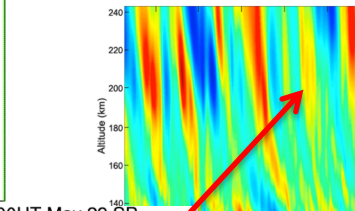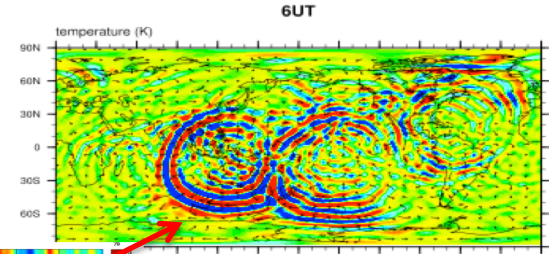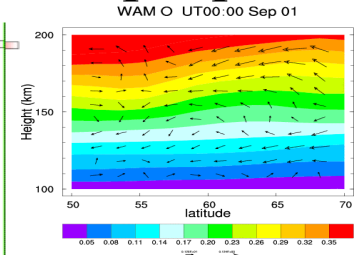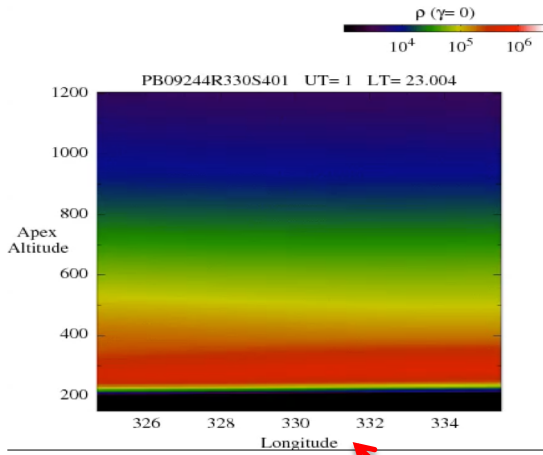
Tropospheric sources drive concentric circle waves in neutral winds, temperature and plasma density

WAM fields spawn ionospheric irregularities with no additional seeding Retterer, Boston College

Arecibo Ne perturbations Djuth et al.

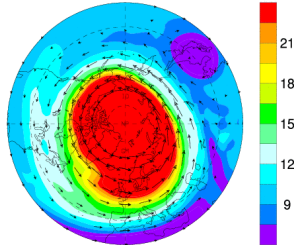Observations: TEC Perturbations undulations in plasma
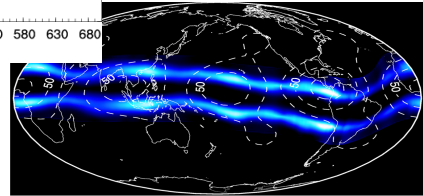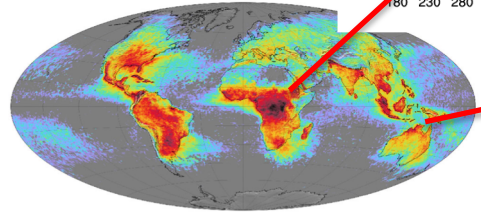
Tropical convection drives plasma longitude structure

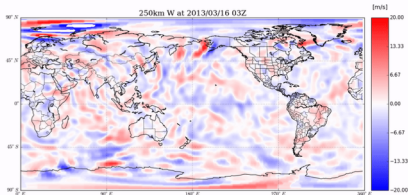*Azeem et al.* 2015

62

Sources from the Lower Atmosphere

- Longitude structure of tropical convection modulates non-migating tidal modes (DE3, DE2), which drive winds and electrodynamics in lower thermosphere dynamo region


Jan 10 UT00 840K PV North

- Changes in stratospheric circulation (e.g., sudden stratospheric warmings) modulating semi-diurnal migrating tidal modes, which also drive electrodynamics

Mar 20N UT00 285km
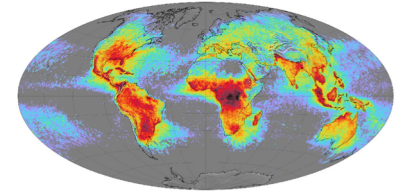
- Midnight temperature and density maxima (MTM, MDM) modulates temperature and density structure, wind reversals, and direct impact on F-region ionosphere

250km W at 2013/03/16 03Z
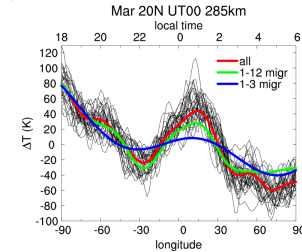
- Spectrum of waves from lower atmosphere driving wind, temperature, and composition variability directly impacts the ionosphere and electrodynamics, including possible triggering of ionospheric irregularities

New Theories for Phase and Intensity Metrics

- Rino's power law (weak) scintillation theory implies, in scale-free limit $q_0 \rightarrow 0$:

$$ROTI^2(\delta t) \sim \frac{c^2}{\delta t^2} C_p G \left[\frac{1}{2\pi} \frac{2\Gamma(3/2-\nu)}{\Gamma(\nu+1/2)(2\nu-1)2^{2\nu-1}} \right] \cdot \left| V_{eff} \delta t \right|^{2\nu-1}, \quad \frac{1}{2} < \nu < \frac{3}{2}$$

(Carrano et al., 2019

$$\sigma_\varphi^2(\tau_c) = \frac{2}{2\nu-1} C_p G \frac{\sqrt{\pi}\,\Gamma(\nu)}{(2\pi)^{2\nu+1}\Gamma(\nu+1/2)} \cdot \left| \tau_c V_{eff} \right|^{2\nu-1}, \quad \frac{1}{2} < \nu$$

(Carrano et al., 2016

$$S_4^2 = C_p \,\wp(\nu) \frac{\Gamma[(5/2-\nu)/2]}{2^{\nu+1/2}\sqrt{\pi}\,\Gamma[\nu/2+1/4](\nu-1/2)} \rho_F^{2\nu-1}, \quad \frac{1}{2} < \nu < \frac{5}{2}$$
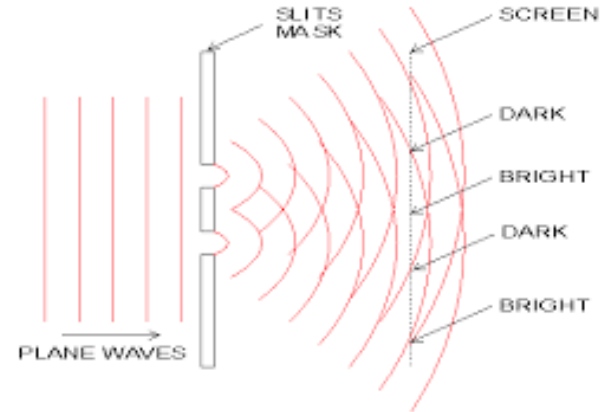
(Rino, 1979)

where

C_p – phase spectral strength

$\wp(\nu)$ –geometry and propagation factor

ν - related to irregularity spectral index as $p(3)=2\nu+1$

G – phase enhancement factor due to geometry

ρ_F – Fresnel scale $\quad \rho_F = \sqrt{\lambda z_R \sec\theta/(2\pi)}$

Γ – gamma function

- Phase metrics (ROTI, σ_φ) depend on effective scan velocity to the power $2\nu+1$.
- Intensity metric (S_4) depends on Fresnel scale to the power $2\nu+1$.
- All three metrics depend on irregularity strength in the same way.

Summary and Conclusions

- The thermosphere and ionosphere is a tightly coupled collision dominated gravitationally-bound system forced by the Sun, the magnetosphere, and waves propagating from the lower atmosphere
- The neutral thermosphere is 99.9% of the mass of the upper atmosphere between 100 to 600 km altitude
- Plasma replaces water vapor or ozone as the important minor species, compared with the lower atmosphere
- The upper atmosphere is non-linear but appears non-chaotic, unlike the lower atmosphere, except for the forcing from the lower atmosphere

- Questions?
- Email tim.fuller-rowell@noaa.gov

Heliophysics Summer School I-T

Storm-Time Electrodynamics: disturbance dynamo

Blanc and Richmond (1980) theory:

- Equatorward winds drive zonal winds at mid-latitude through the action of the Coriolis force
- Zonal winds $\rightarrow$ equatorward Pedersen current
- Equatorward wind $\rightarrow$ equatorward Hall current
- Positive charge builds up at the equator producing a poleward directed electric field which balance the wind driven equatorward current
- Eastward Hall current causes +ve charge build up at the dusk terminator and -ve charge build-up at dawn
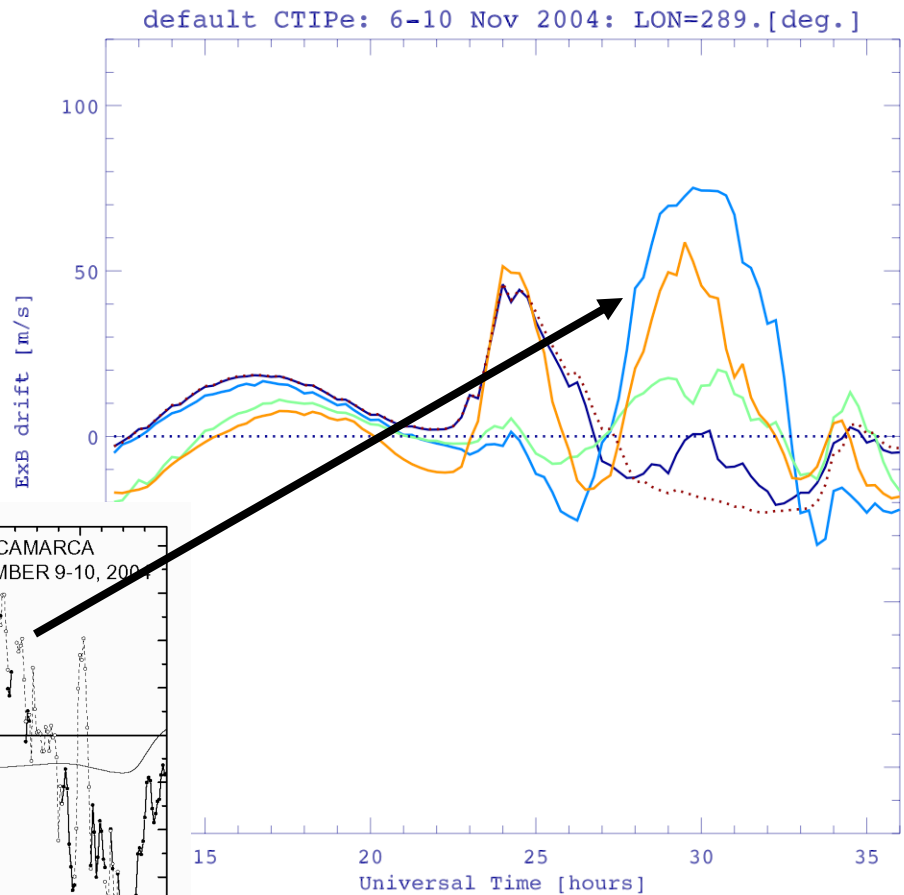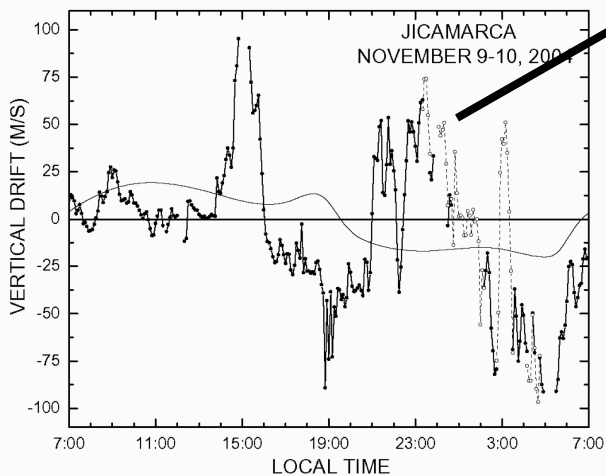- Reverse S_q

$$J_{\vartheta u} = -\frac{\sigma_1}{\sin I} u_\phi B + \sigma_2 u_\theta B$$

$$J_{\phi u} = \sigma_1 \sin I u_\theta B + \sigma_2 u_\phi B$$

$$J_{\theta E} = \frac{\sigma_1}{\sin I} E_\varepsilon + \frac{\sigma_2}{\sin I} E_\phi$$

$$J_{\phi E} = -\sigma_2 E_\varepsilon + \sigma_1 E_\phi$$
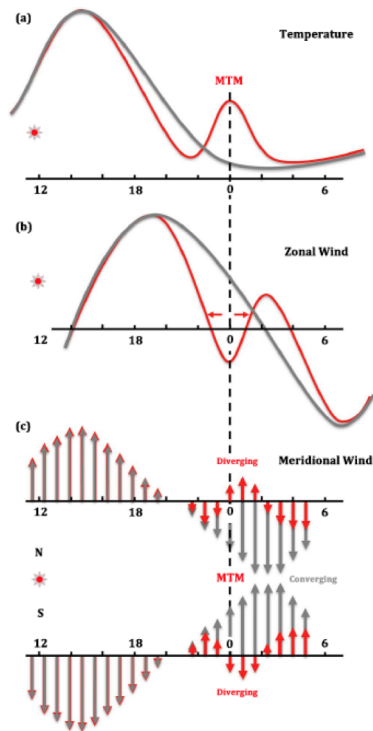
CTIPe simulation of disturbance dynamo

default CTIPe: 6-10 Nov 2004: LON=289.[deg.]

JICAMARCA
NOVEMBER 9-10, 200[...]

68
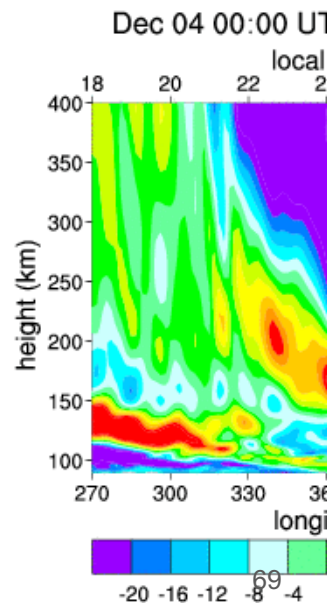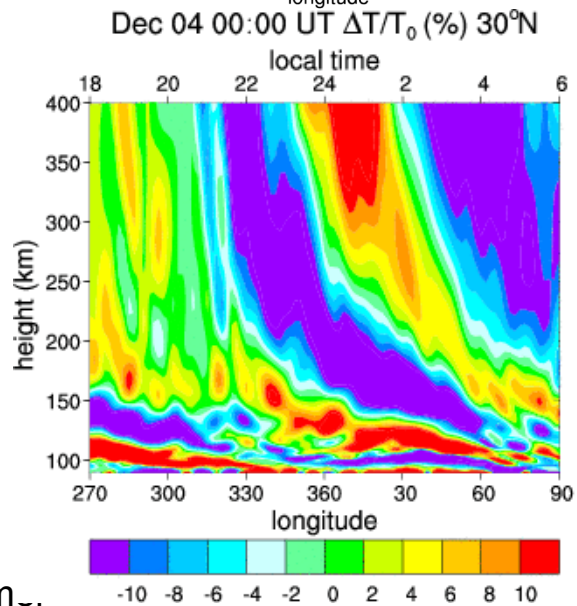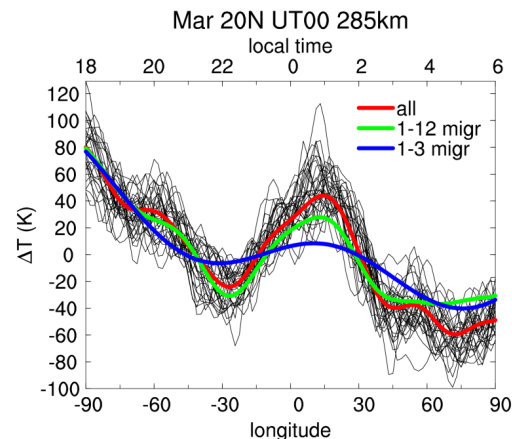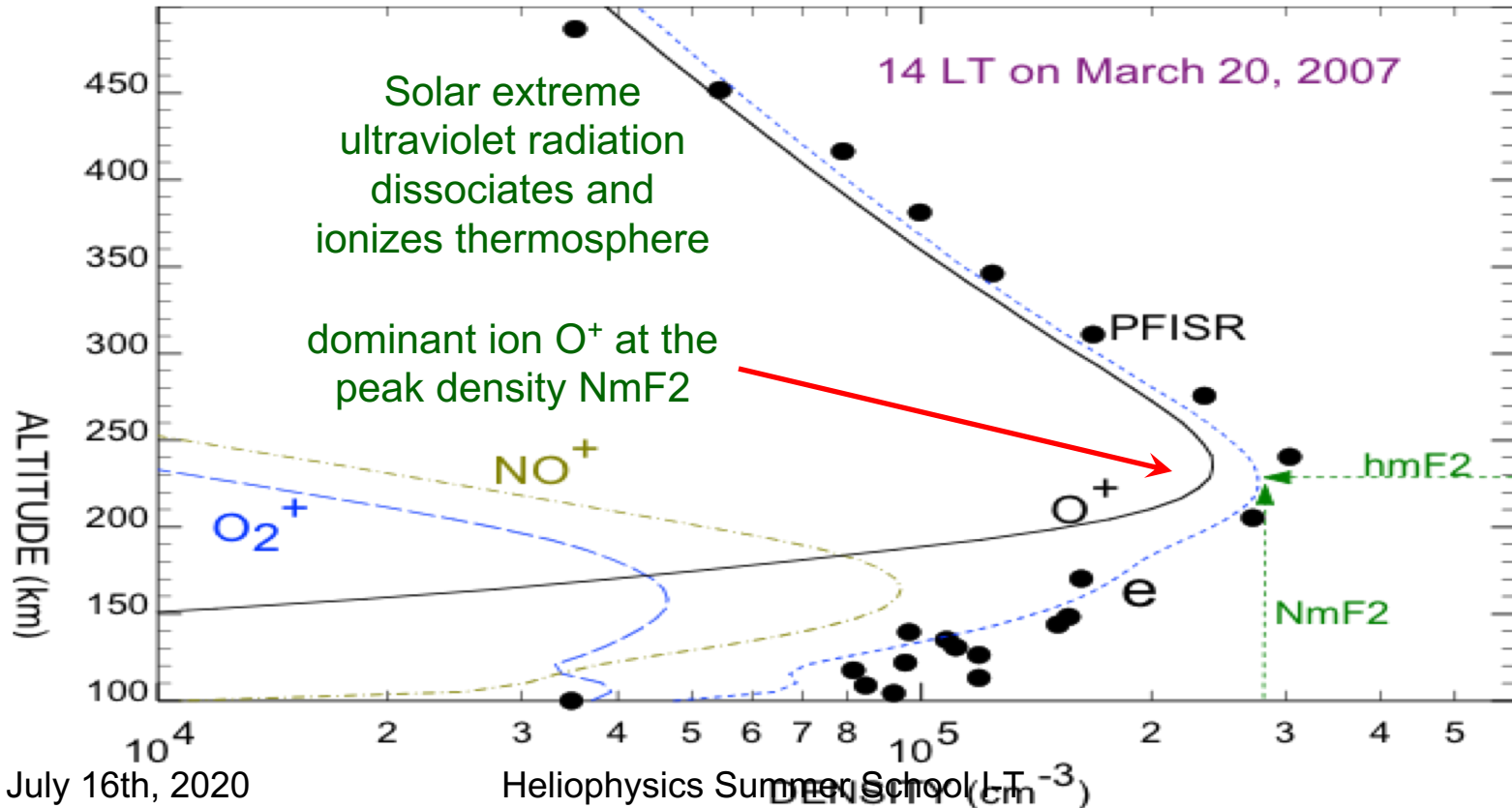
Midnight Temperature Maximum (MTM)

Figure 4. Schematic plot of local time variations of neutral temperature, zonal wind, and meridional wind with MTM (red lines and arrows) and without MTM (gray lines and arrows).

Mar 20N UT00 285km

Dec 04 00:00 UT $\Delta T/T_0$ (%) 30°N

Dec 04 00:00 UT

Plasma densities from IPE Ionosphere Model

July 16th, 2020   Heliophysics Summer School LT   70

Thermosphere-Ionosphere Responses to Magnetospheric Sources

- Auroral precipitation enhances conductivity at high latitudes

- Magnetospheric electric fields enhances plasma transport at high latitudes

- Magnetospheric "penetration electric fields" imposed globally in less than a second

- Ion drag drives high latitude wind system up to ~ 1 km/s

- Joule and particle energy heats atmosphere

- Thermal expansion, neutral density increase, horizontal pressure gradients, equatorward wind surges

- Changes in global circulation

- Neutral composition changes

- Disturbance dynamo

- Positive and negative ionospheric storm phases

Neutral Dynamics in pressure coordinates

$$\frac{\partial}{\partial t}V_\theta = -\frac{V_\theta}{r}\frac{\partial}{\partial\theta}V_\theta - \frac{V_\phi}{r\sin\theta}\frac{\partial}{\partial\phi}V_\theta - \omega\frac{\partial}{\partial p}V_\theta - \frac{g}{r}\frac{\partial}{\partial\theta}h +$$

horizontal and vertical advection   pressure

$$\left(2\Omega + \frac{V_\phi}{r\sin\theta}\right)V_\phi\cos\theta + g\frac{\partial}{\partial p}\left[(\mu_m + \mu_T)\frac{p}{H}\frac{\partial}{\partial p}V_\theta\right] - \nu_{ni}\left(V_\theta - U_\theta\right)$$

(13)
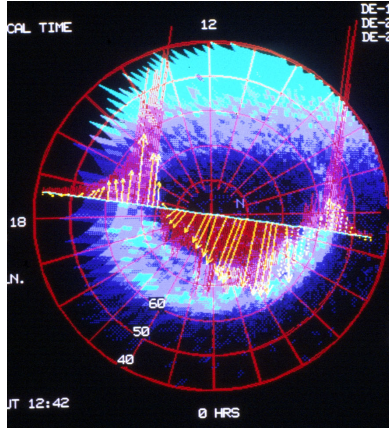
Coriolis and "curvature"   vertical viscosity   ion drag

and

$$\frac{\partial}{\partial t}V_\phi = -\frac{V_\theta}{r}\frac{\partial}{\partial\theta}V_\phi - \frac{V_\phi}{r\sin\theta}\frac{\partial}{\partial\phi}V_\phi - \omega\frac{\partial}{\partial p}V_\phi - \frac{g}{r\sin\theta}\frac{\partial}{\partial\phi}h -$$

$$\left(2\Omega + \frac{V_\phi}{r\sin\theta}\right)V_\theta\cos\theta + g\frac{\partial}{\partial p}\left[(\mu_m + \mu_T)\frac{p}{H}\frac{\partial}{\partial p}V_\phi\right] - \nu_{ni}\left(V_\phi - U_\phi\right)$$

(14)

Geomagnetic Forcing on the T-I system
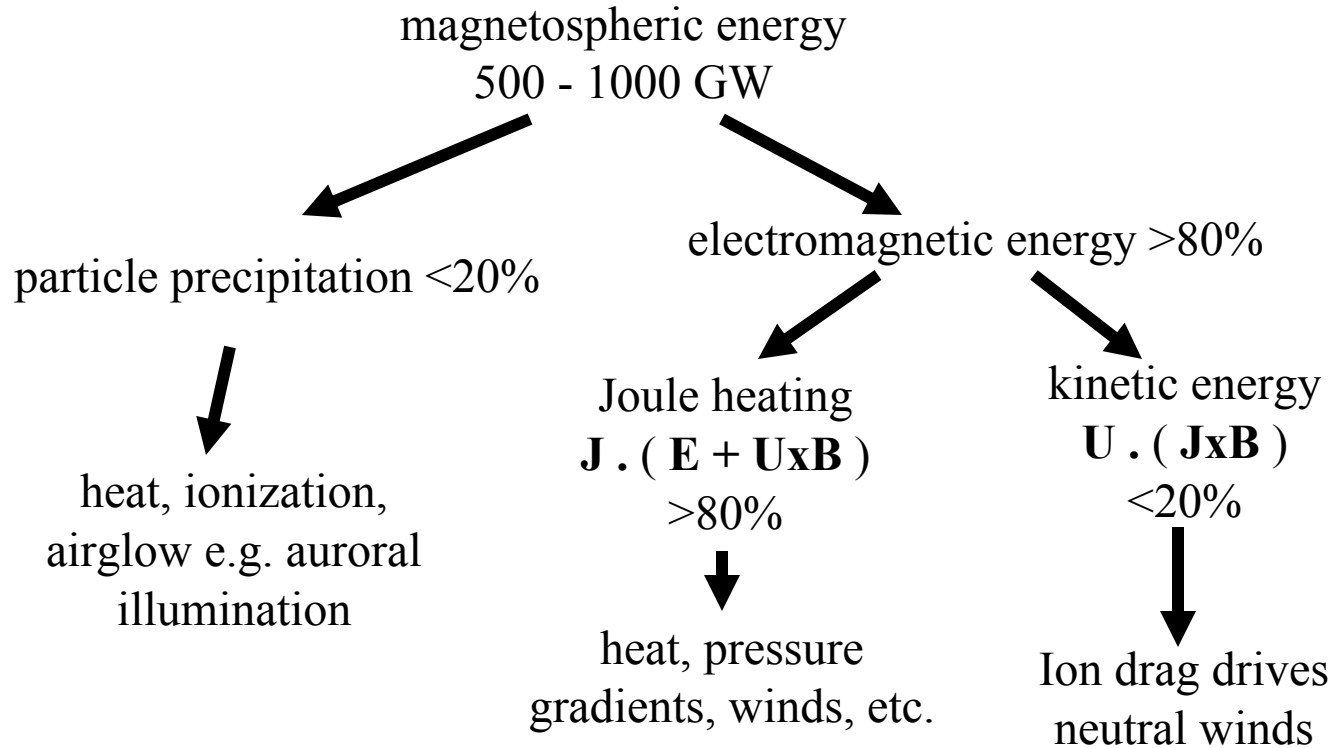

Dynamics Explorer

Stan Solomon

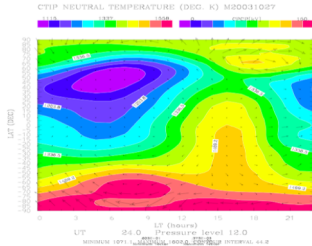**Enhanced Electric Field and Ion Drag**

Enhanced Auroral Precipitation and Ionospheric Conductivity

Joule Heating $\quad Q_J \propto \sigma \vec{E}^2$

Ion Drag $\quad \vec{F} \propto \sigma(\vec{U}_I - \vec{V}_n) \equiv \sigma(\frac{\vec{E}x\vec{B}}{B^2} - \vec{V}_n)$

Energy Flow

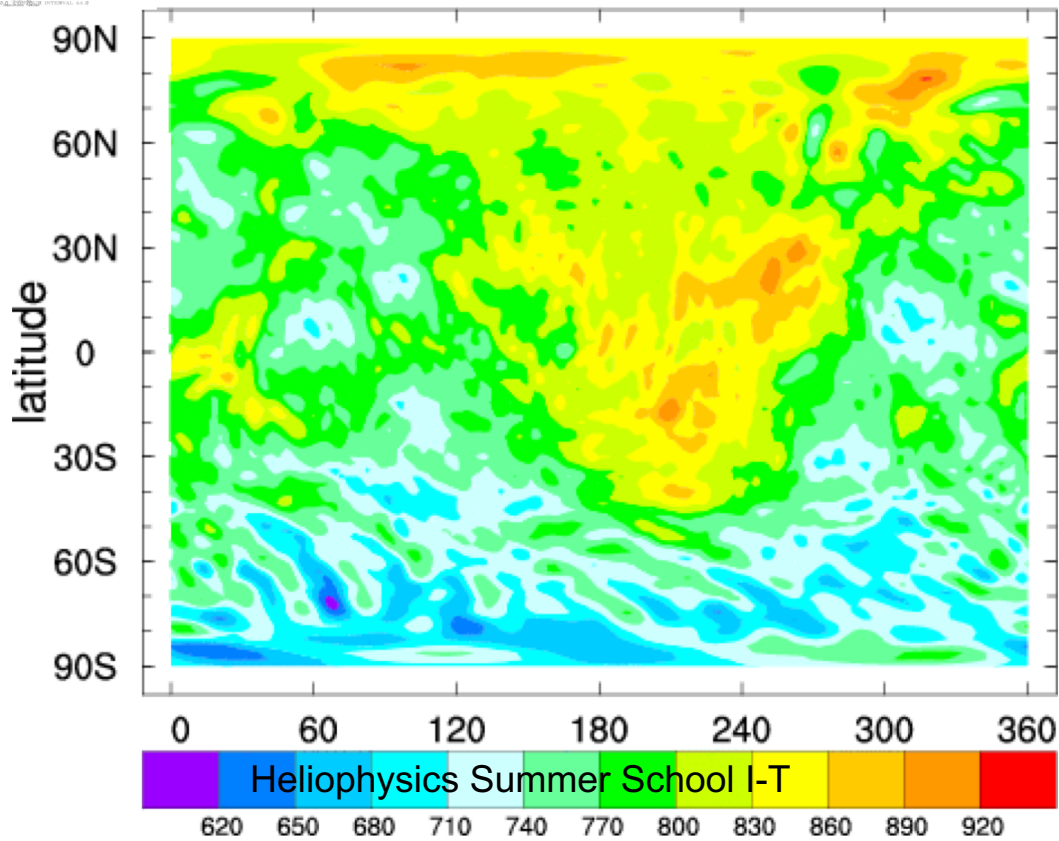magnetospheric energy
500 - 1000 GW

particle precipitation <20%

electromagnetic energy >80%

heat, ionization,
airglow e.g. auroral
illumination

Joule heating
$J . (E + UxB)$
>80%

kinetic energy
$U . (JxB)$
<20%

heat, pressure
gradients, winds, etc.

Ion drag drives
neutral winds

….is this reality?

Sep 03 UT00:00 200km WAM T

Temperature 200 km altitude

….or is it this ?

Heliophysics Summer School I-T

620 650 680 710 740 770 800 830 860 890 920
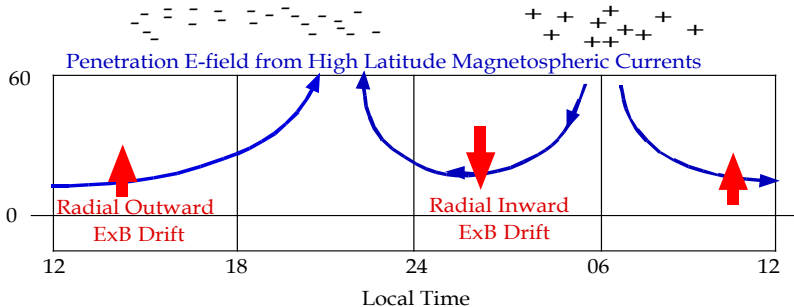
July 16th, 2020
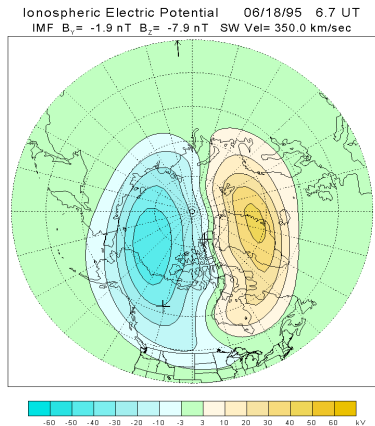
Magnetospheric Forcing

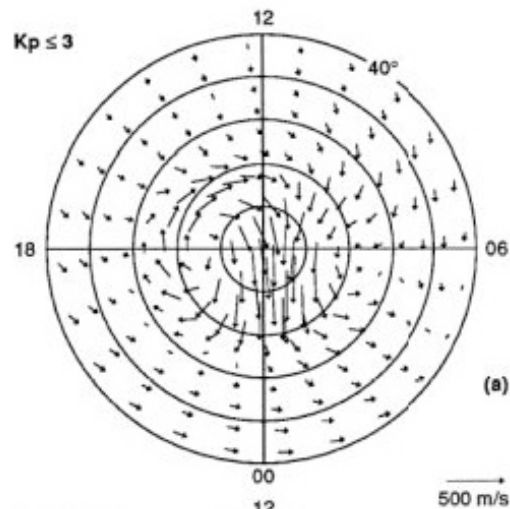TIROS/NOAA auroral precipitation patterns driven by power index:
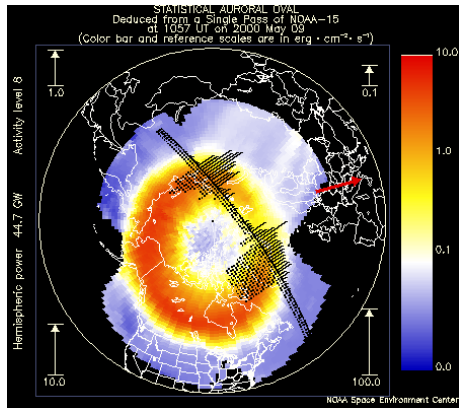
Weimer electric field patterns driven by solar wind data:
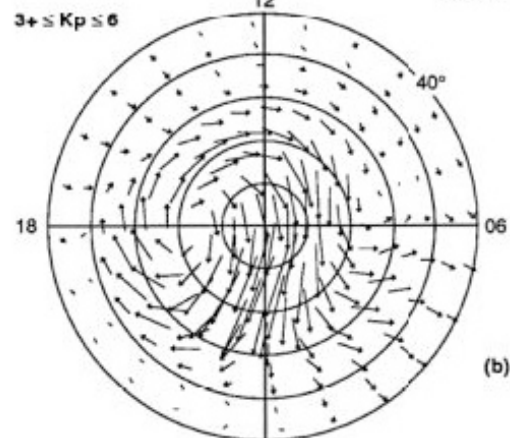

Joule heating
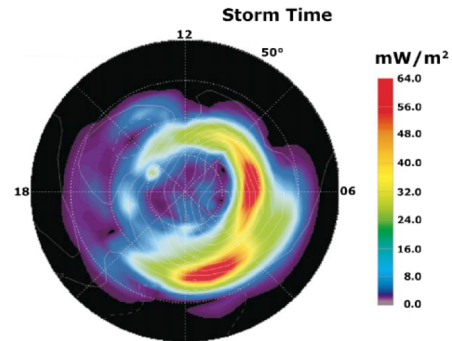
Neutral Winds in Quiet and Active Conditions

Clear asymmetry in
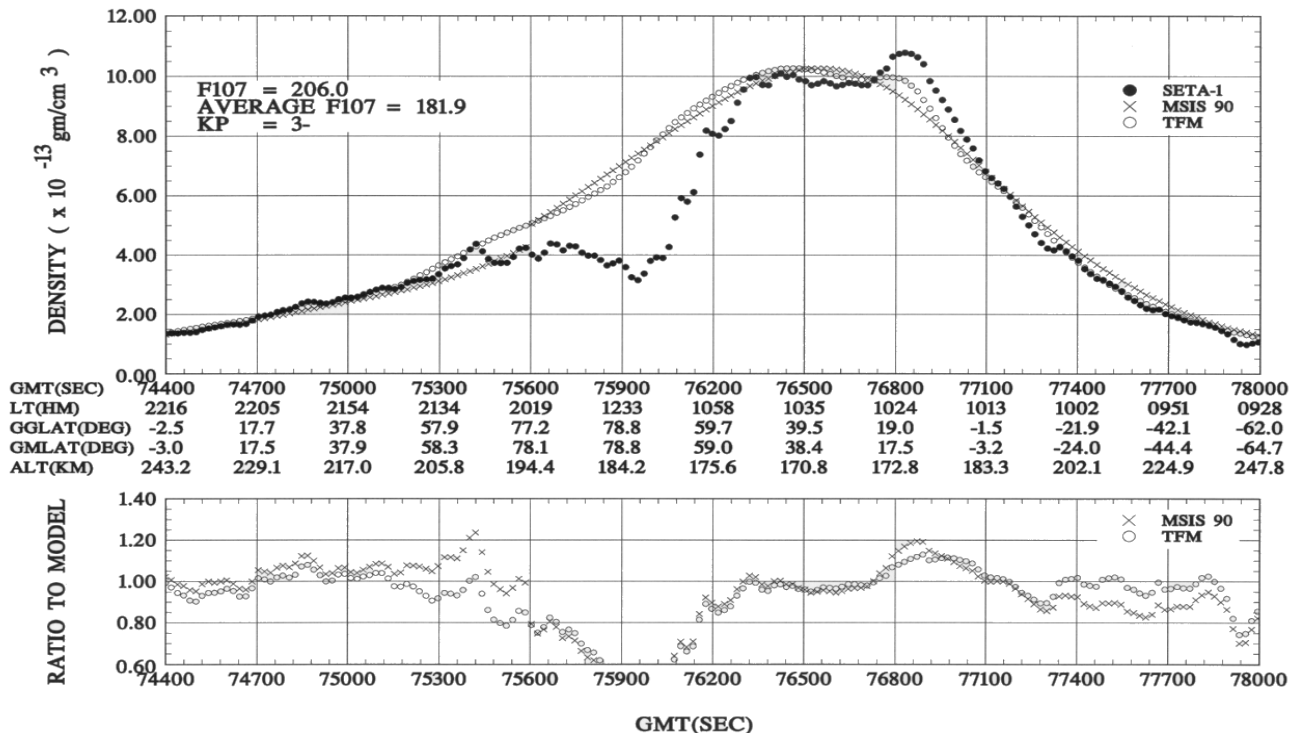response in dawn and
dusk sector of auroral
oval

Quiet

Active

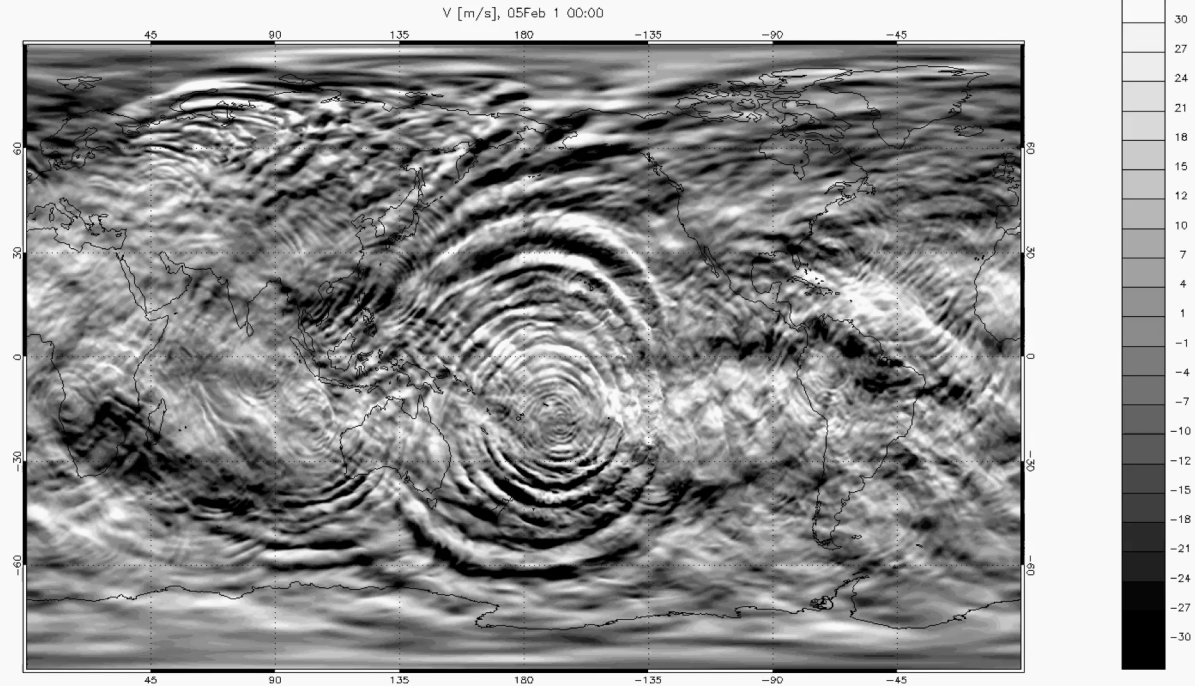# Neutral density holes - dynamically driven?

SETA-1 DENSITY DATA
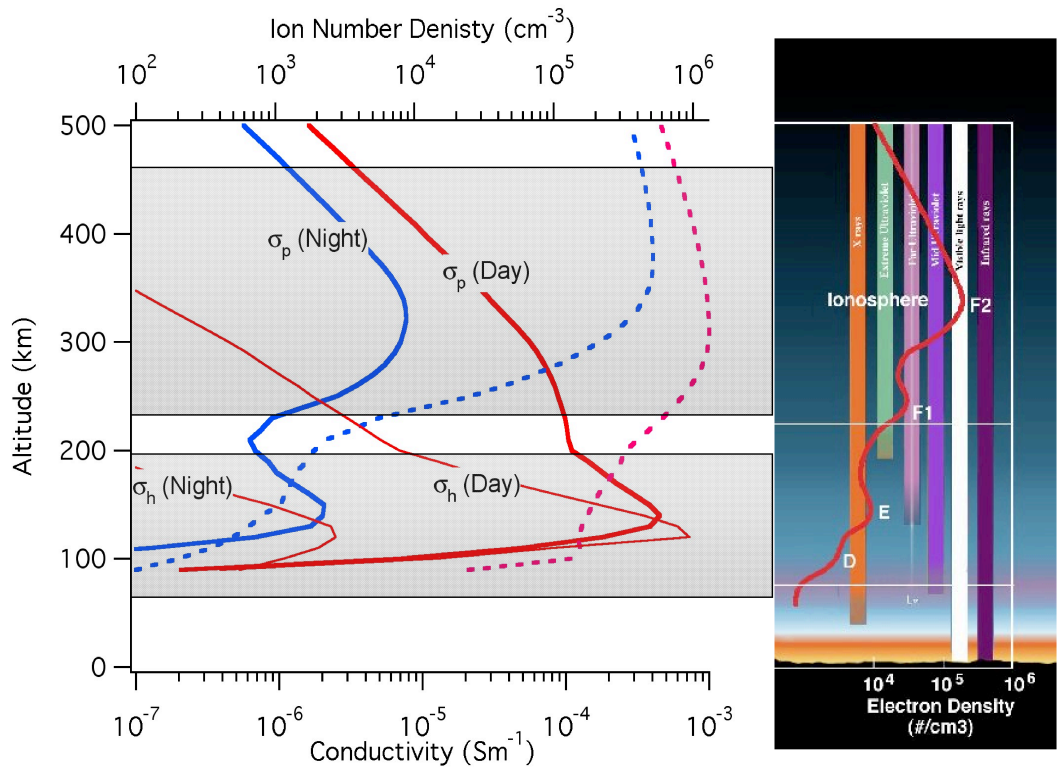DAY 79093
ORBIT NO. 294

WACCM meridional winds, ~110 km
25 km horizontal, 1/10 scale height vertical resolution

V [m/s], 05Feb 1 00:00

Courtesy Hanli Liu

Pedersen and Hall Conductivity

Kinetic Energy Spectrum

The dynamical core of the NWS Global Forecast System (GFS) spectral weather model and WAM is fairly diffusive

The NWS has recently replaced the dynamic core of the weather model with a Finite-Volume Cubed-Sphere (FV3)

FV3 is much less diffusive, so retains power at the shorter wavelength, and is non-hydrostatic

WAM will adopt the new FV3 non-hydrostatic dynamical core so will retain a richer more complete spectrum of waves penetrating to the upper atmosphere